T.C.
ISTANBUL UNIVERSITY-CERRAHPASA
INSTITUTE OF GRADUATE STUDIES

M.Sc. THESIS

PRODUCTION OF SMART MATERIALS FOR STENT APPLICATIONS

FADİ BAGHDADİ

SUPERVISOR
Prof. Dr. İlven MUTLU

Department of Nanoscience and Nanoengineering

Nanoscience and Nanoengineering Programme

ISTANBUL- August, 2021

This study was accepted on 26/8/2021 as a M. Sc. thesis in ....., ... by the following Committee.

Examining Committee Members

Prof. Dr. İlven MUTLU(Supervisor)
İstanbul University-Cerrahpaşa
Faculty of Engineering

Prof. Dr. Gülin Selda POZAN SOYLU
İstanbul University-Cerrahpaşa
Faculty of Engineering

Assist. Prof. Dr. Sefa ÇELİK
İstanbul University
Faculty of Science

As required by the 9/2 and 22/2 articles of the Graduate Education Regulation which was published in the Official Gazette on 20.04.2016, this graduate thesis is reported as in accordance with criteria determined by the Institute of Graduate Sttudies by using the plagiarism software to which Istanbul University-Cerrahpasa is a subscriber.

This thesis is supported by the project numbered 35631 of Istanbul University-Cerrahpaşa Scientific Research Projects Executive Secreteriat.

FOREWORD

I would like to thank my family members who have always supported me

August 2021 Fadi Baghdadi

TABLE OF CONTENTS

Page

LIST OF FIGURES

Page

LIST OF TABLES

Page

LIST OF SYMBOLS AND ABBREVIATIONS

Symbol	Explanation
T	**:** Temperature
t	**:** Time
º	**:** Degree
α	**:** Alpha
β	**:** Beta

Abbreviation	Explanation
g	**:** Gram
mg	**:** Mili gram
mm	**:** Mili meter
nm	**:** Nano meter
ppm	**:** Parts per million
PVA	**:** Polyvinylalcohol
µm	**:** Micro meter
MA	**:** Mechanical alloying
OCP	**:** Open circuit potential

ÖZET

YÜKSEK LİSANS TEZİ

STENT UYGULAMALARI İÇİN AKILLI MALZEMELERİN ÜRETİLMESİ

FADİ BAGHDADİ

İstanbul Üniversitesi-Cerrahpasa

Lisansüstü Eğitim Enstitüsü

Nanobilim ve Nanomühendislik Anabilim Dalı

Danışman : Prof. Dr. İLVEN MUTLU

Bu tez çalışması kapsamında, koroner stent kullanımı için polimer matrisli kompozit ve metalik çeşitli akıllı malzemelerin geliştirilmesi, üretimi ve incelenmesi gerçekleştirilmiştir. Takviyeli polimer matrisli kompozit malzemelerin üretiminde kullanılan kalıplar stereolitografi esaslı eklemeli imalat yöntemi ile üretilmiştir. Daha sonra aljinat kalıplama ile takviye edilmiş polimer matrisli kompozit ürünler üretilmiştir. Şekil bellekli TiNi tozu, karbon nano tüp (CNT) tozu, ve karbon siyahı tozu ile takviye edilmiş polimer matrisli kompozit malzemeler kalıp boşluğuna dökülmüştür. Ayrıca mekanik metamalzeme şekilli, şekil bellekli TiNi tozu, karbon nano tüp (CNT) tozu, ve karbon siyahı tozu takviyeli epoksi veya poliüretan matrisli kompozit malzeme üretimi de gerçekleştirilmiştir. Ayrıca, kendi-kendini onarma davranışı gösteren polimer matrisli kompozit malzemeler üretilmiş ve kendi kendini onarma özellikleri incelenmiştir. Şekil bellekli Fe esaslı alaşımlar ve Ti-Ni esaslı alaşımlar ise toz metalurjisi yöntemi ile stent uygulamaları için üretilmiştir. Numunelerin mekanik özellikleri ve mikroyapıları araştırılmıştır. Ayrıca, numunelerin elastisite modülü ve kendi-kendini onarma özelliklerinin incelenmesinde tahribatsız ultrasonik muayene yönteminden yararlanılmıştır.
Temmuz 2021, 62. sayfa.

Anahtar kelimeler: Şekil bellek, akıllı malzeme, toz metalurjisi, metamalzeme, stent

SUMMARY

M.Sc. THESIS

PRODUCTION OF SMART MATERIALS FOR STENT APPLICATIONS

FADİ BAGHDADİ

Istanbul University-Cerrahpasa

Institute of Graduate Studies

Department of Nanoscience and Nanoengineering

Supervisor : Prof. Dr. İLVEN MUTLU

In this thesis, development, production and characterization of several polymer matrix composite and metal based smart materials for coronary stent applications were done. Moulds, which were used in the production of reinforced polymer matrix composites, were produced by stereolithography based additive manufacturing method. Then, the polymer matrix composite materials were produced by alginate molding. Shape memory TiNi powder, carbon nano tube (CNT) powder, and carbon black powder reinforced polymer matrix composite materials were poured into the mould. In addition, mechanical metamaterial shaped TiNi powder, carbon nano tube (CNT) powder, and carbon black powder reinforced epoxy and polyurethane matrix composites were manufactured. In addition, polymer matrix composite materials with self-healing behaviour were produced and their self-healing behaviour was investigated. Shape memory Fe based alloys and Ti-Ni based alloys were produced by powder metallurgy technique for stent applications. Microstructure and mechanical properties of the materials were studied. In addition, nondestructive ultrasonic tests were used in order to characterize the elastic modulus and self-healing behaviour of the specimens.

August 2021, 62. pages.

Keywords: Shape memory, smart material, powder metallurgy, metamaterial, stent

1. INTRODUCTION

1.1. SMART MATERIALS

In general, smart materials are a relatively novel group of advanced engineering materials, which have very important engineering applications. Fabrication and characterization of the smart materials is a new area in the engineering science. Smart materials are fabricated to make a response in a controlled and adjusted way. Smart materials can be employed in the actuator applications, in the sensor applications, or as an artificial muscle in the robotic applications [1].

Metamaterials can be desribed as an artificial materials, which can not found in the nature. Metamaterials are synthetic materials. Behaviours of the metamaterials can be attributed to their geometry, but not their intrinsic material properties or chemical content. Meta-materials can be decribed as s macroscopic composite materials with 3-dimensional, cellular architecture designed to produce optimized properties [1].

Metamaterial based smart materials can be subdivided as;

- Mechanical metamaterials (auxetics) having negative Poisson's ratio
- Electronical/magnetical type metamaterials having negative diffraction index

Figure 1.1 shown below illustrates the behaviours of the non-auxetic and auxetic metamaterial under tensile and compression forces (loads) [3].

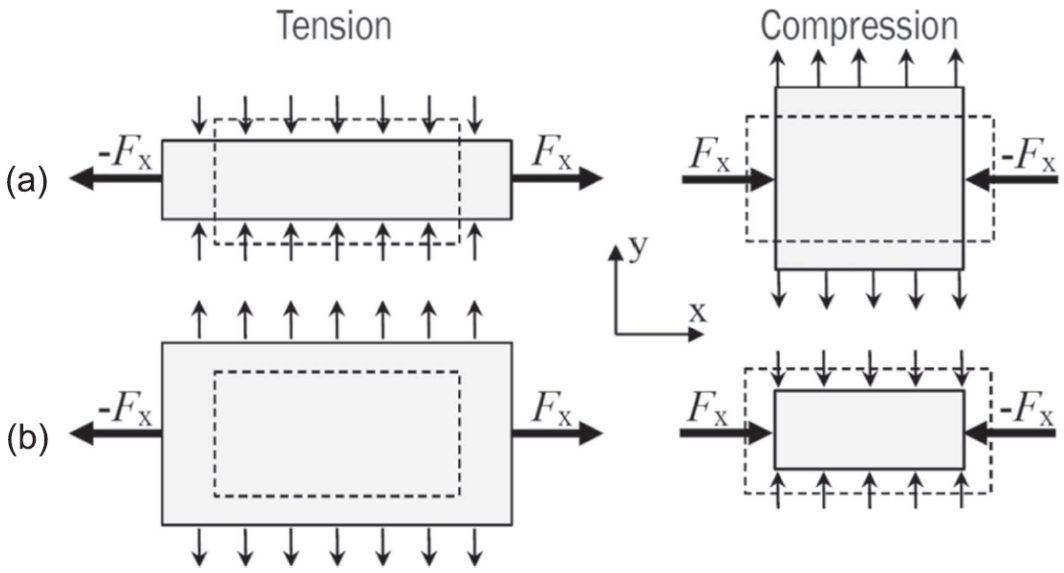

Figure 1.1: Non-auxetic and auxetic mateials under tensile and compression loads [3]

Figure 1.2 shown below illustrates the re-entrant auxeticand chiral auxetic geometries [3]

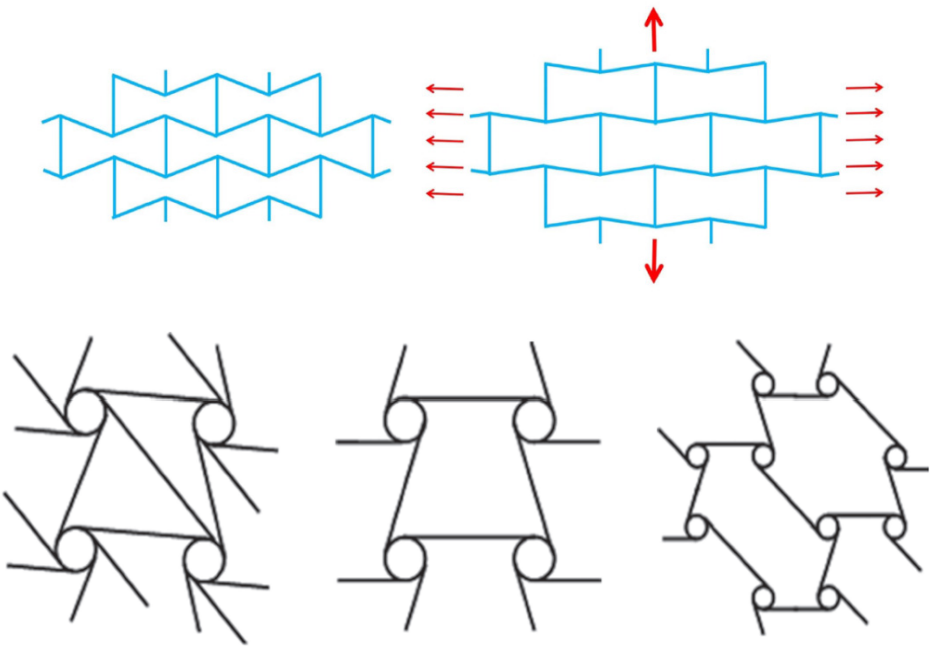

Figure 1.2: Re-entrant auxetic and meta-chiral structures [3]

Figure 1.3 illustrates a coronary stent (in heart) or peripheral stent (in esaphagus tube) applications of the mechanical metamaterials (auxetic materials). In general, the auxetic behaviour provides a radial strength to the coronary or peripheral stents [3].

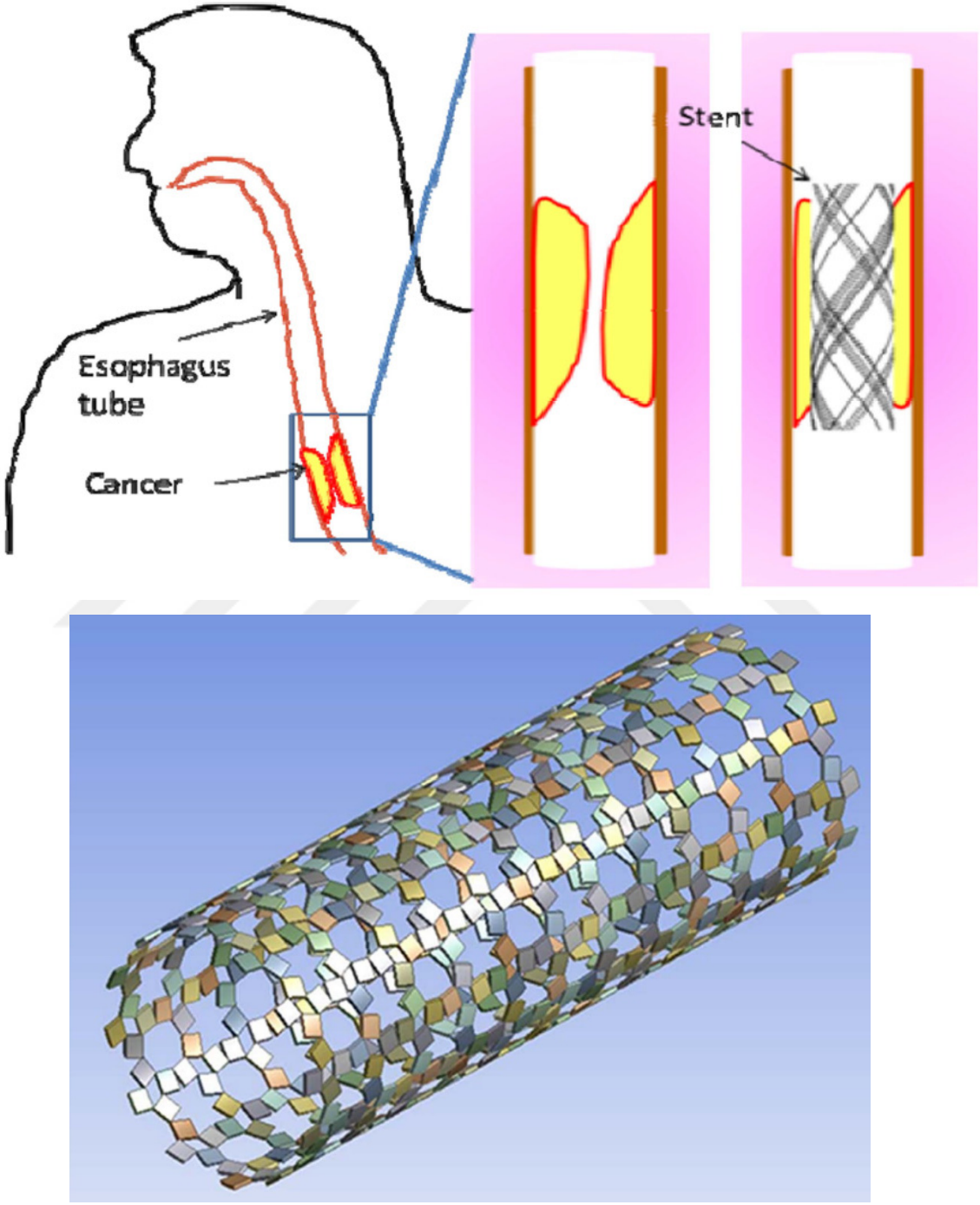

Figure 1.3: Auxetix stent application [3]

1.2. SHAPE MEMORY MATERIALS

In general, shape memory alloys are gruop of advanced engineering materials and show shape recovery behaviour to their pre-deformed first shape by heating or by removal of stress. In general, nitinol (Ni-Ti) based alloys are the most commonly used and well-known shape memory alloy group for their relatively low phase transformation temperature and also relatively high shape memory recovery. But, on the other hand, Cu based shape memory alloys and Fe based shape memory alloys can be also employed in some applications. In general, the shape memory (recovery) effect is due to diffusionless solid to solid thermoelastic-martensitic phase transformation. Deformation mode of the martensite phase is by twinning instead of more common slip mechanism [4].

In general, for the shape memory behavior, plastic deformation must be by twinning mechanism not by slip mechanism of dislocations, and martensitic phase transformations must be thermoelastic but not non-thermoelastic, and lastly there must be an orientation (crystallographic). In the shape memory alloys, there are 3 main phases; first is twinned martensite, second is detwinned martensite and the last one is austenite. If the shape memory materials is deformed in the martensitic phase, the material can return to pre-deformed initial shape after heating to the high temperature austenitic phase region. In general, deformation occur by two mechanisms/modes (slip or twinning). In the slip mechanism, the grain boundaries are deformed and shape of the sample is permanent. On the other hand, in the twinning mode, deformation is reversible. So, the twinning is the deformation mechanism in the shape memory effect. Shape memory materials are transformed to the martensite phase by twinning mechanism. After force is applied to the sample the alloy transform to the martensite, twins are reoriented to produce de-twinning structure. The twin boundaries have low energy and high mobility. So, shape recovery is easy.

There are 2 types of composition invariant transformations. First is short range diffusional massive transformation, in which there is no orintation. Atoms move individually. Second is martensitic transformation, in which phase transformation involves crystallographic relationship between austenite and martensite phases.

At the beginning, when there is no load, the shape memory alloy is in the austenite phase at high temperature (first point). From the first to the second points, temperature decreases and the alloy transformed to martensite. Transformation mode of the martensşte is twinning. Then, from point 2 to point 3, load (stress) is applied to the alloy and de-twinning ocuurs (de-twinned martensite phase formed). From point 3 to point 4, the load is removed and elastic deformation (strain) is recovered. In the point 4, the alloy is deformed (plastic deformation) in the de-twinned martensite phase. From point 4 to point 1, the lloy is heated to the austenite phase and the alloy remember its first shape and then recover. Figure given below illustrates the shape memory effect (SME).

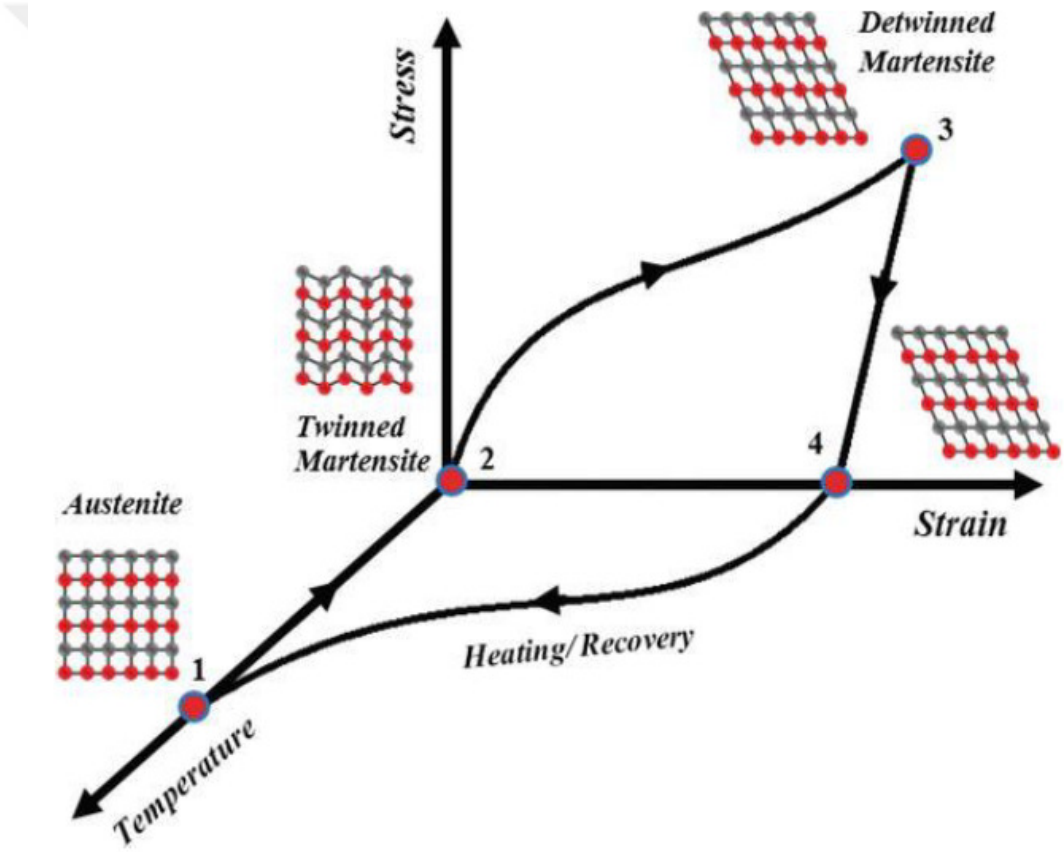

Figure 1.4: Shape memory effect [2]

In the martensitic phase transformation, there must be undistorted surface between martensite and austenite phases. The strain must be reduced in order to enhance nucleation of the martensite phase. Figure given below schematically illustrates the a) martensite phase transformation mechanism, b) slip mechanism, c) twinning mechanism in the metals.

Reversible martensitic phase transformations are subdivided to 2 main groups as first is thermoelastic and second is non-thermoelastic transformations. The non-thermoelastic transformations occuır mainly in the ferrous alloys. Thermoelastic transformations occur mainly in the shape memory alloys. Shape memory effect (SME) is associated by the crystallographic reversibility.

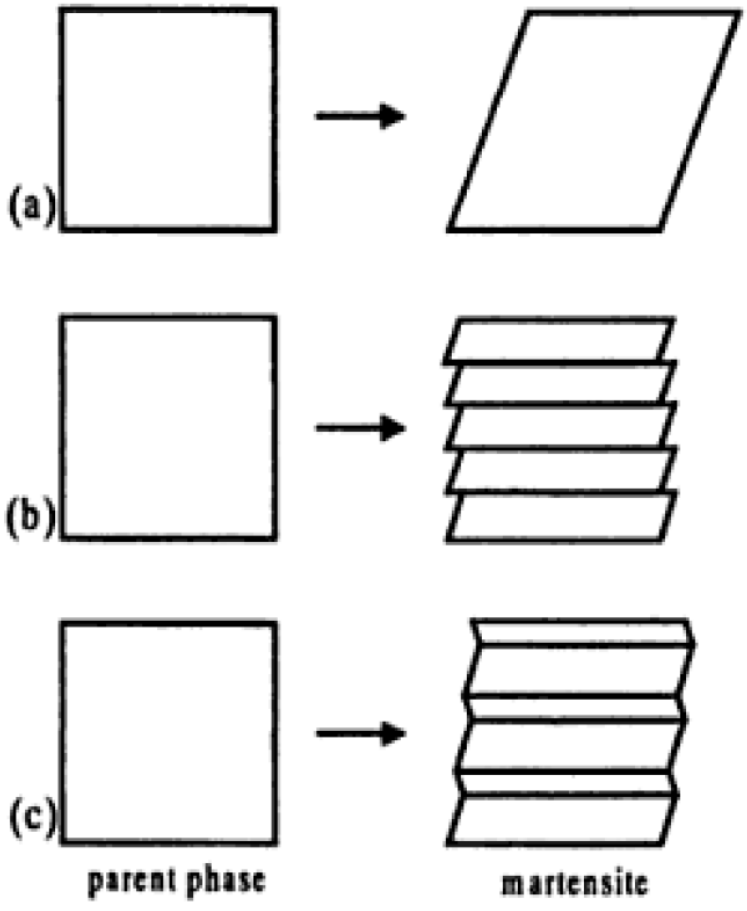

Figure 1.5: a) Martensite transformationb) slip, c) twinning [2]

Traditional Shape Memory Effect

Figure 1.6 given below illustrates the one-way shape memory effect in the stress-strain graph in the alloys. In general, de-twinning and the reorientation behaviours are very important in the shape memory alloys [5].

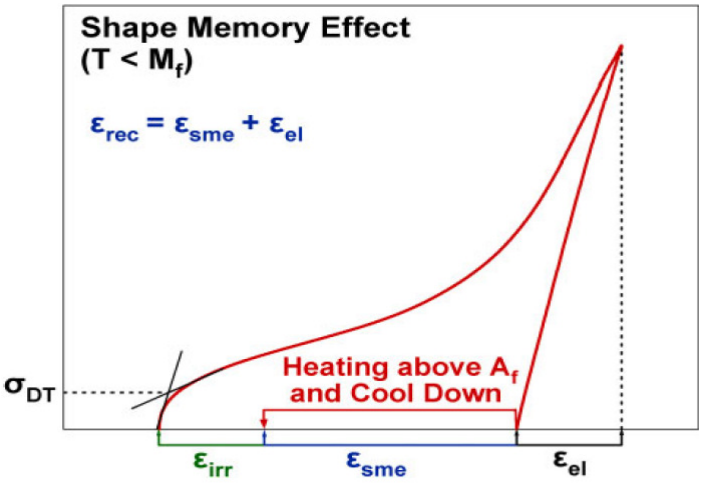

Figure 1.6: One-way shape memory effect [5]

Superelasticity (Pseudoelasticity)

Superelasticity (pseudoelasticity) is a type of shape memory alloy (SMA). Superelasticity (pseudoelasticity) can be described as stress-induced transformation based shape memory.

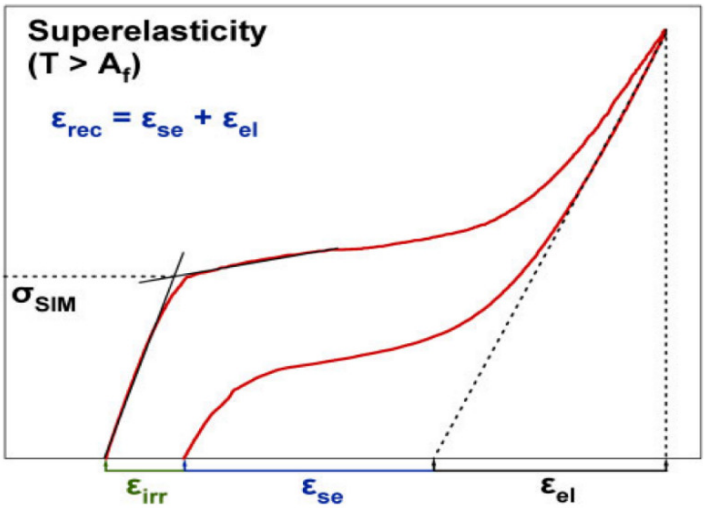

Figure 1.7: Superelastic properties [5]

Nitinol (Ni-Ti)

Nitinol is a popular advanced material in the engineering applications. Nitinol (Ni-Ti alloys) shows shape memory effect and superelasticity (pseudoelasticity) effect. Usually, nitinol includes nickel (Ni) and titanium (Ti) elements at the equal atomic percentage. Properties of the Ni-Ti can be controlled by aging and cold working. As the Ni content of the material raises in the NiTi alloys, phase transformation temperature decreases dramaticly. Aging of the NiTi alloys leads to precipitation of very fine Ni-based precipitates in the microstructure, which decrease the Ni content of the matrix and raise the transformation temperature of the alloy. Moreover, fine Ni-based precipitates can increase the strength of the alloy. Usually, Ni-rich NiTi alloys are stronger. Phase transformation temperature of the shape memory alloys is very important in the development and design of shape memory products as the control and adjusting mechanisms of the products are depend on the phase transformation temperature. In automobile applications, space applications, and aviation applications, the phase transformation temperature must be high (higher than 100 ºC). NiTi alloys having lower phase transformation temperature are not suitable for the high temperature applications.

Table 1.1: Properties of the NiTi [4]

Property	Symbol	Units	Value	
			Martensite	Austenite
Corrosion Resistance	–	–	Similar to 300 series SS or Ti-alloy	
Density	ρ_D	kg/m^3	6450–6500	
Electrical Resistivity (approx.)	ρ_R	μΩ cm	76–80	82–100
Specific Heat Capacity	c	J/kg K	836.8	836.8
Thermal Conductivity	k	W/m K	8.6–10	18
Thermal Expansion Coefficient	α	m/m K^{-1}	6.6×10^{-6}	11.0×10^{-6}
Ultimate Tensile Strength	σ_{UTS}	MPa	895 (Fully annealed)/1900 (Hardened)	
Young's Modulus (approx.)	E	GPa	28–41	75–83
Yield Strength	σ_Y	MPa	70–140	195–690
Poisson's Ratio	ν	–	0.33	
Magnetic Susceptibility	χ	μemu g	2.5	3.8

Fe-Based Shape Memory Alloys

In general, the overall shape memory behaviour of the Fe-based alloys are lower than NiTi based shape memory alloys or Cu-based shape memory alloys. But, Fe-based shape memory alloys are cheaper than Cu-based and NiTi-based alloys.

There are two types of Fe-based shape memory alloys; Fe-Ni based shape memory alloys and Fe-Mn-Si based shape memory alloys.

Fe-Mn-Si shape memory alloys are promising alloys in the advanced engineering applicationd, espessialy with Ni, Co or Cr additions. Alloying additions to the Fe-Mn-Si alloys enhance the mechanical properties. These alloys have higher hysteresis. In the Fe-Mn-Si based shape memory alloys there are different martensitic transformations such as face-centered cubic (FCC) to body-centered cubic (BCC) or body-centered tetragonal (BCT), face-centered cubic (FCC) to face-centered tertagonal (FCT), or face-centered cubic (FCC) to hexagonal-close packed (HCP). In the Fe-Mn-Si based alloys high temperature austenite phase transforms to martensite (HCP) at room temperature. Stress-induced martensitic phase transformation in the Fe-Mn-Si based shape memory alloys occurs by creation of stacking faults.

As in the Fe-Mn-Si based shape memory alloys there is a face-centered cubic (FCC) to hexagonal-close packed (HCP) transformation, in the Fe-Ni based shape memory alloys there is face-centered cubic (FCC) to body-centered tetragonal (BCT) phase transformation. Although Fe-Mn-Si based shape memory alloys are used in industrial applications, Fe-Ni based shape memory alloys are not used in industrial applications yet. In the Fe-Ni based alloys shape memory effect is small due to non-thermoelastic transformation [1-5].

Shape Memory Polymers

Shape memory polymers are smart material based stimuli-responsive material. Shape memory polymers can remember their first shape/dimentions after fixing the temporary shape. In general, shape memory polymers consist of a switching phase (reversible phase) and a net point. The swithcing phase usually fix the temporary phase. The net point (fixing phase) can be restore the permanent phase. Switching phases are fabricated by using thermoplastic polymers. Fixing phase is fabricated by chemical or physical cross-link network polymers. In the shape memory polymers, general mechanism for the shape memory can be attributed to 2 phase structure.

- Fixing phase (hard segment), which can return the permanent shape.
- Reversible phase (soft segment), which can fix the temporary shape.

In general, chemical crosslinks (covalent bonds) and physical crosslinks construct the hard phase. Physical crosslinks can be seen in polymers with crystalline and amorphous regions. Figure shown below illustrates the general shape memory mechanism in the polymers [1]

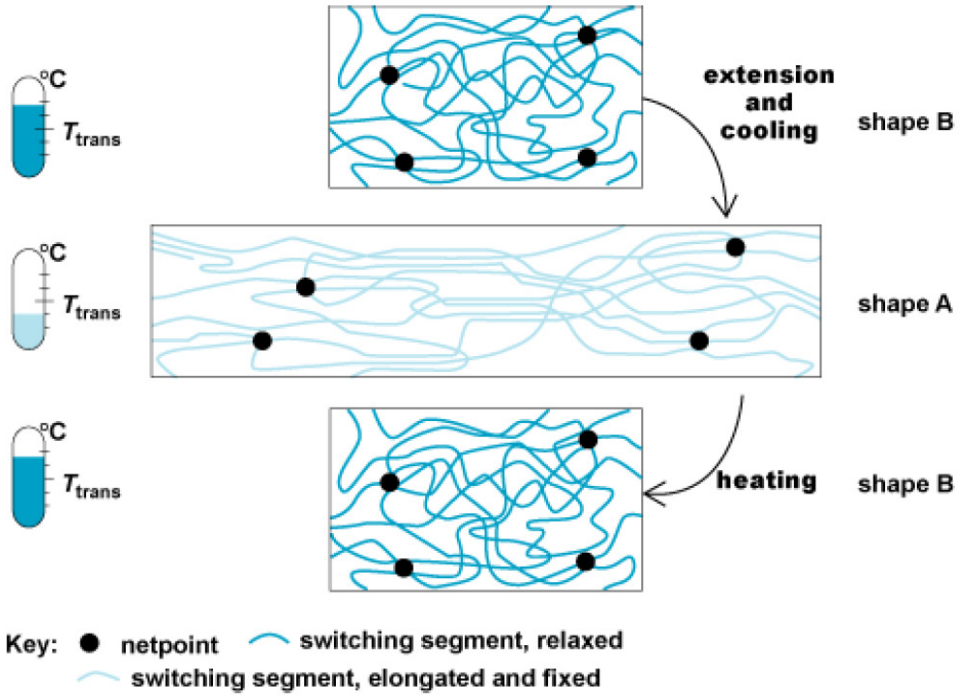

Figure 1.8: Shape memory mechanism in polymers [1]

1.3. SELF HEALING MATERIALS

Self-healing can be described as the property of a group of engineering material that enables to heal micro-cracks (defects) intrinsically. The self-healing can occur automatically without any intervention. This automatic (self-triggered) self-healing can be described as autonomous self healing (self-healing without intervention). On the other hand the non-autonomous self-healing occurs with external triggering (heat, light, magnetic field, electric field) [5-7].

There are two types of self healing behaviour. First is extrinsic based self-healing (added). Second self-healing type is intrinsic based self-healing. In the intrinsic type self-healing, there is need to any material for healing.

Classification of the Self-Healing Mechanisms

- Microcapsules based
- Hollow Fibers based
- Microvascular Network based

Figure 1.9 given below illustrates the self-healing behaviours/mechanisms of some polymer materials by using embedded healing materials (also polymer based) [7].

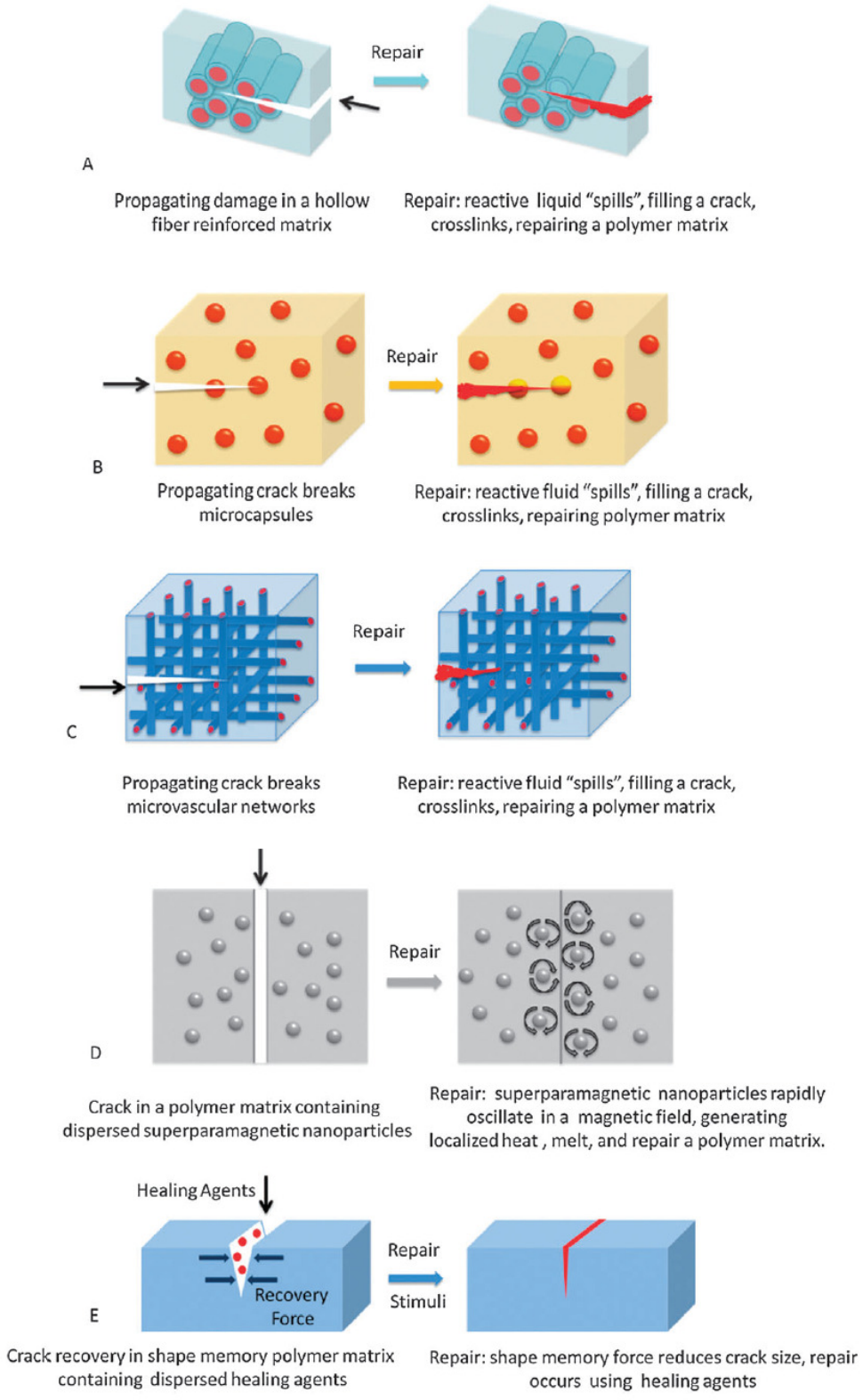

Figure 1.9: Self-healing of the polymers [7]

1.4. CORONARY STENTS

A stent is a very small hollow tube-shaped medical device. Usually, stents can be employed in the angioplasty applications in order to open the closed veins in the arters of the heart. In addition, stents can be also used in the other regions of the body (such as peripheral stents) [8-11].

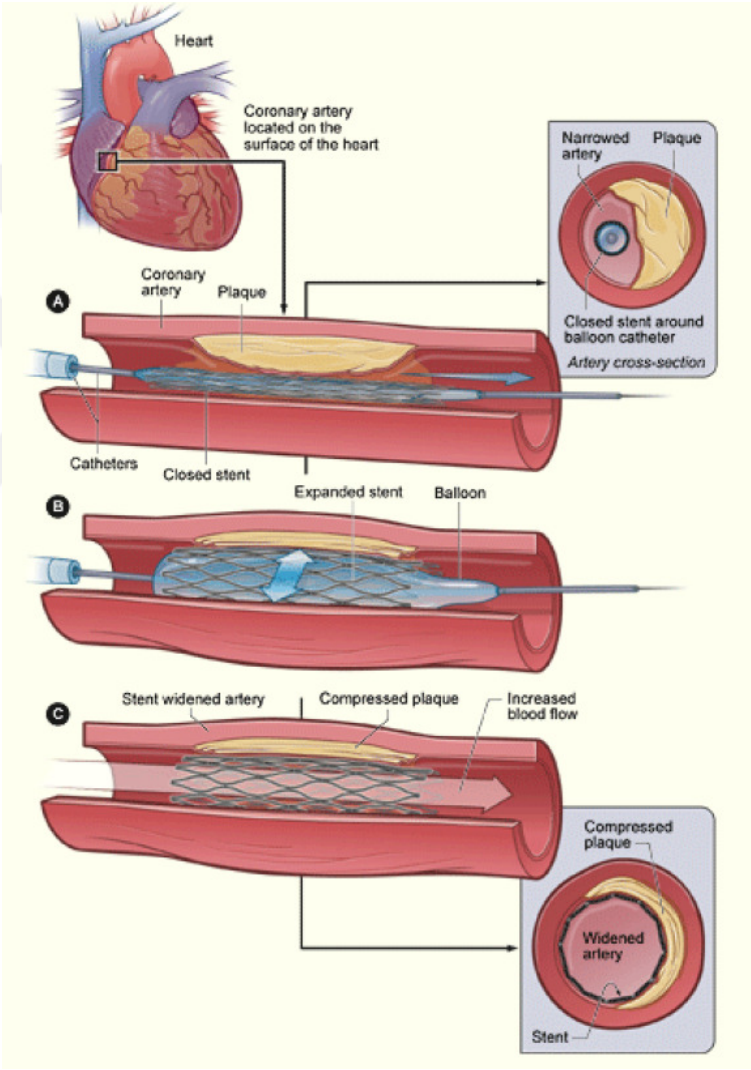

Figure 1.10: Placement of a stent [8]

The SEM images given below shows the main fabrication steps of a typical coronary stent device. In general first step is fabrication of a mini-tube with about 3mm diameter. Second step is laser-cutting of the mini-tube. Then, annealing and laser cuting of the mini-tube. Last step is descaling and finishing.

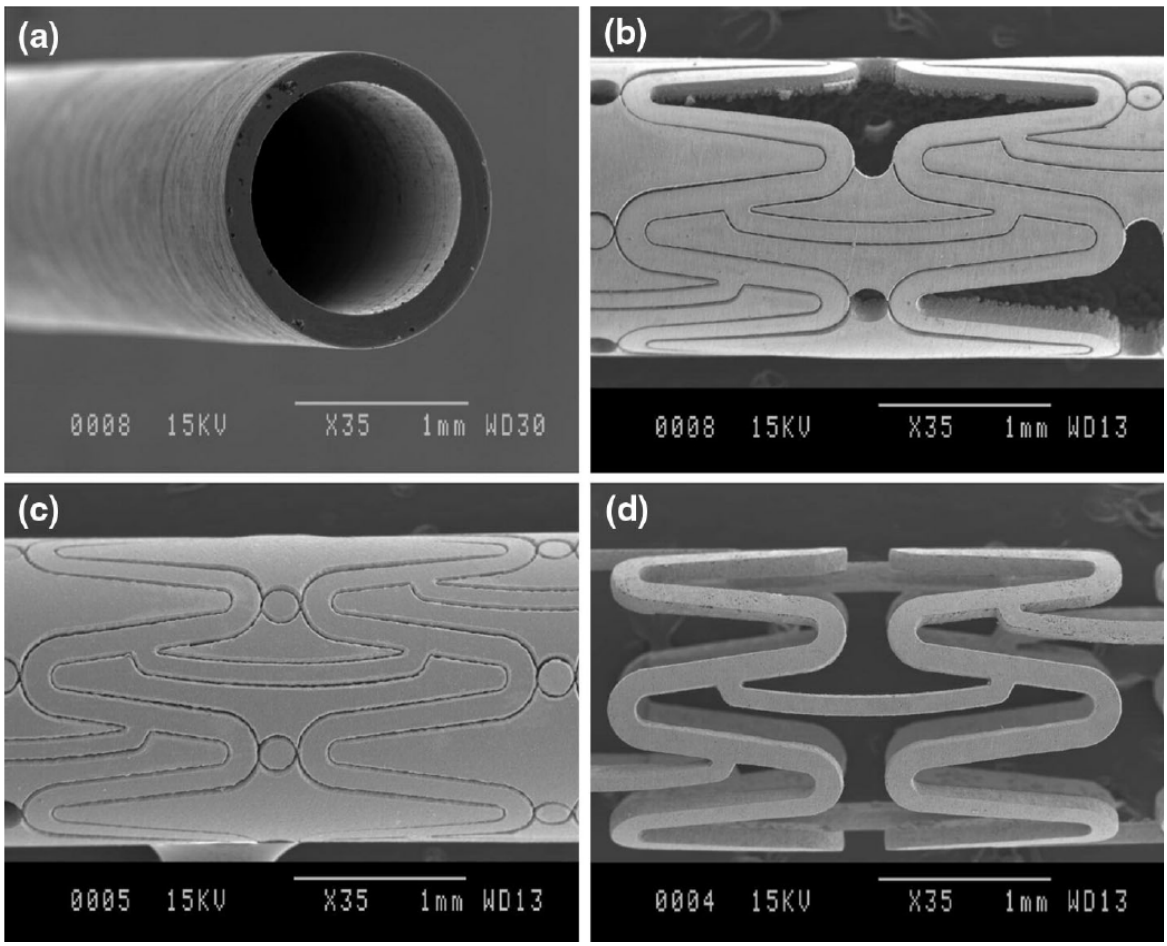

Figure 1.11: Production steps of a stent [9]

1.5. LITERATURE REVIEW

Fu et al. [10] were studied Fe-Ni-Co based shape memory alloys. The authors were enhanced the superelasticity of the Fe-Ni-Co alloys by microstructure and texture control (grain orientation). The authors were studied the effects of col-rolling, annealing, solution and recrystallization on the shape memory behaviour.

Tanaka et al [11] were studied Fe-Ni-Co-Al based superelastic alloys. The solution temperature, hardness and martensite phase transformation temperatures of the alloys were investigated. The specimens were manufactured by induction melting under argon. Then, the Fe-Ni-Co-Al based alloy ingots were hot rolled. The alloys were finally aged.

Drucekr et al. [12] were produced and investigated Fe-Mn-Si and Fe-Mn-Si-Cr-Ni based shape memory alloy couplings. Fe-Mn-Si and Fe-Mn-Si-Cr-Ni based shape memory alloy specimens were produced by casting in sand moulds. Then, the shape memory specimens were rolled and annealed. The amount of shape recovery of the shape memory specimens was found to be suitable for several industrial applications.

Aydoğmuş [13] was studied porous TiNi alloys with porosities in the range 21%-81% produced by powder metallurgy fabrication route in which magnesium was used as space holder material. The processed alloys showed interconnected open macro-pores. The author was found that porosity have no effect on the phase transformation temperatures of the alloys. Porous Ti-Ni shape memory alloys showed suitable superelasticity and shape memory behavior for industrial applications.

Lee [14] was studied shape memory polymers. Thermal stimuli-responsive shape memory polymers based on blends of thermoplastic polyurethane (TPU) and polycaprolactone (PCL) were studied. Mechanical, thermal, rheological and morphological properties of the blends are characterized. Shape memory properties are also studied with the fold deploy shape memory test.

Söyler [15] was studied production of Fe-Mn-Si shape memory alloys by advanced powder metallurgy methods. Production of shape memory alloys with different amounts of Fe, Mn and Si were studied in mechanical alloying tests. In addition, Cr and Ni are added to the alloy to increase the corrosion behaviour of the specimens. Experiments were showed that four hour of mechanical alloying is applicable to the Fe-Mn-Si-Cr-Ni alloys.

Lee et al. [16] were studied the Fe-based shape memory alloy as a strenghening material for reinforced concrete in civil structures. The specimens were investigated by tensile tests. The results of the Fe-based shape memory materials were suitable for applications in the civil structures.

Yuan et al. [17] were fabricated and investigated 3-dimensional printed mechanical metamaterials with high energy absorbtion property. Auxetic materials were provided high energy absorption capacity.

Wang et al. [18] were studied 2-dimensional mechanical metamaterials (auxetics). Auxetic materials show elastic properties in the orthogonal direction to the force. The metamaterials are manufactured by rapid prototyping.

Jabur et al. [19] were fabricated and then characterized the Ni-Ti-Cr based and Ni-Ti-Al based shape memory alloys. The specimens were produced by powder metallurgy method. The transformation temperatures of the Ni-Ti-Cr based and Ni-Ti-Al based shape memory alloys increased with increasing Cr and Al.

Eda et al. [20] were studied Ti-Ni-Co shape memory alloy. The Ti-Ni-Co shape memory alloys were produced by powder metallurgy. Ti-Ni-Co alloys showed higher shape recovery rate than Ti-Ni alloy.

Liu et al. [21] were studied the Fe-Mn-Si based shape memory alloys. Microstructure, yield strength, elastic modulus (Young' modulus), shape recovery properties of the samples were characterized.

2. MATERIALS AND METHODS

2.1. PRODUCTION OF POLYMER MATERIALS

Additive Manufacturing

In the present thesis, stereolithography based additive manufacturing device (Formlabs, USA) was used to produce moulds for the metamaterial-shaped TiNi powder reinforced polymer matrix composite specimens. Figure 2.1 shows the additive manıfacturing device for the production of the moulds.

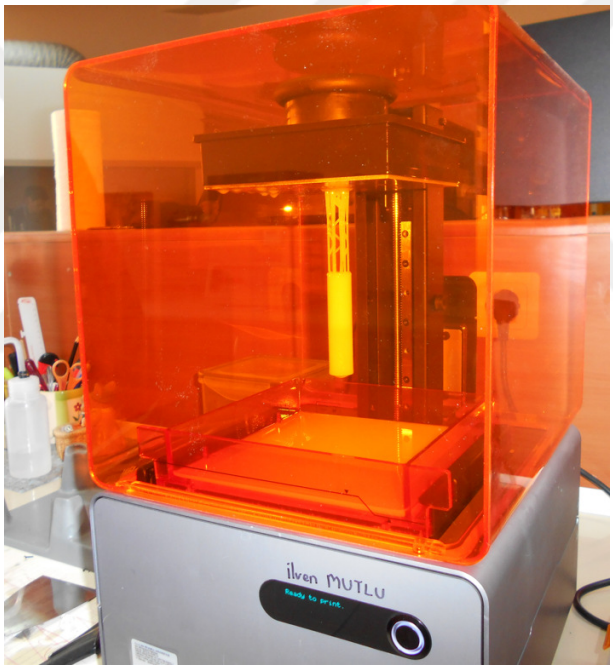

Figure 2.1: Additive manufacturing

Metamaterial Production

Alginate based replica method was used for the production of the metamaterials shaped composite specimens. Alginate was used as a moulding (negative) material. Reinforced polymer matrix composites were poured into the alginate mould and then the metamaterial shaped specimens were obtained.

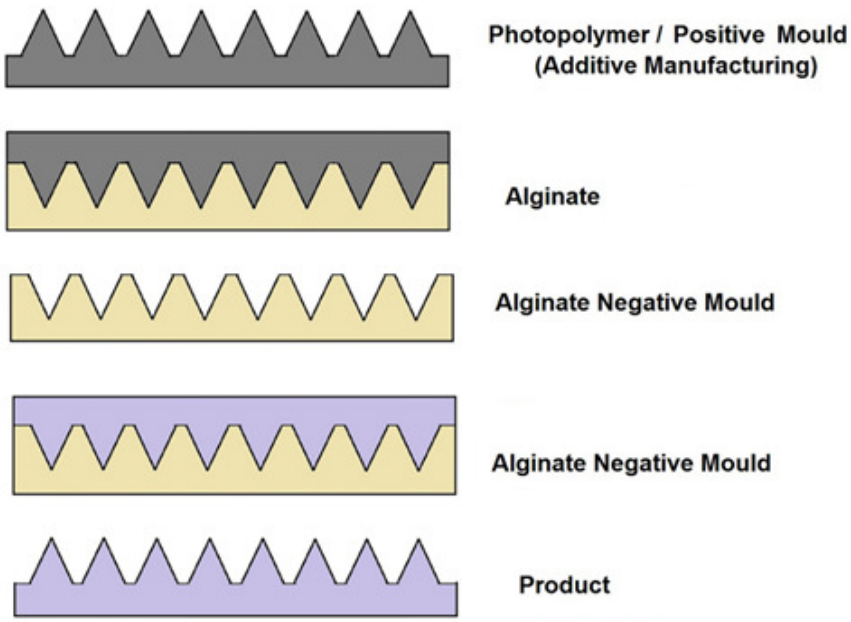

Figure 2.2: Alginate moulding method

Polyurethane Based Composite Specimens

Figure 2.3 illustrates the polymerization of the polyurethane (PU) by mixing 50 % liquid polyol and 50 % liquid isocianate. After mixing the polymer about 4 minutes, the reinforcements (TiNi powder, carbon nano tube (CNT), carnon black) were included to the liquid polymer and lastly the viscous mixture was poured into the mould.

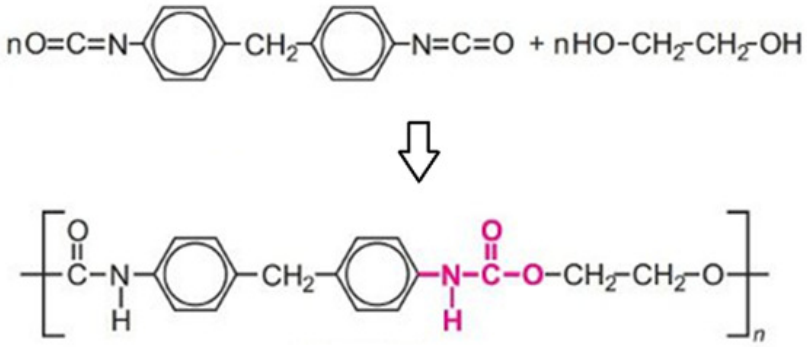

Figure 2.3: Polymerisation mechanism of the polyurethane

Epoxy Based Composite Specimens

Figure 2.4 illustrates the polymerization (cross-linking/hardening) of the thermoset epoxy by mixing 65 wt.% liquid epoxy pre polymer and 35 wt.% liquid hardener. After mixing the polymer about 25 minutes, the reinforcements (TiNi powder, carbon nano tube (CNT), carbon black) were included to the liquid polymer and lastly the viscous mixture was poured into the mould.

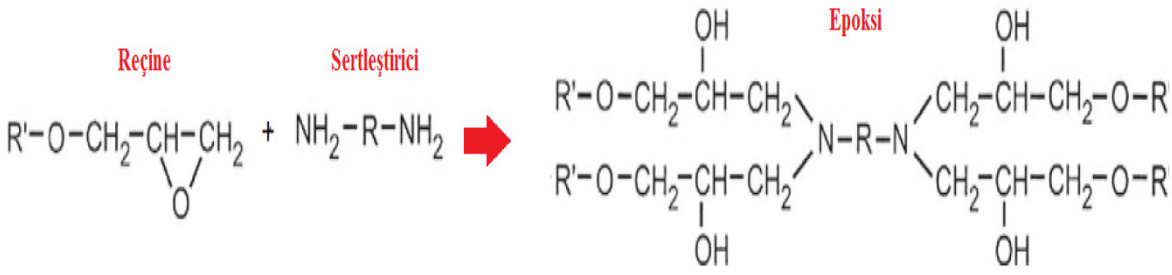

Figure 2.4: Polymerisation (hardening) mechanism of the epoxy

PU-Epoxy Based Self Healing Composite

Initially, polyurethane (PU) based polymer matrix was prepared by by mixing 50 % liquid polyol and 50 % liquid isocianate. Then the polyurethane (PU) mixture was divided into two equal parts. One PU part was mixed with liquid epoxy pre-polymer, and the other PU mixture part was mixed with the liquid hardener of epoxy. Then, the two mixture were mixed together about 2 minutes. Lastly, the two mixtures (PU-epoxy and PU-hardener) were mixed together about 1 minute and then poured into the mould. Figure 2.5 illustrates the PU-epoxy based self-healing composite production steps.

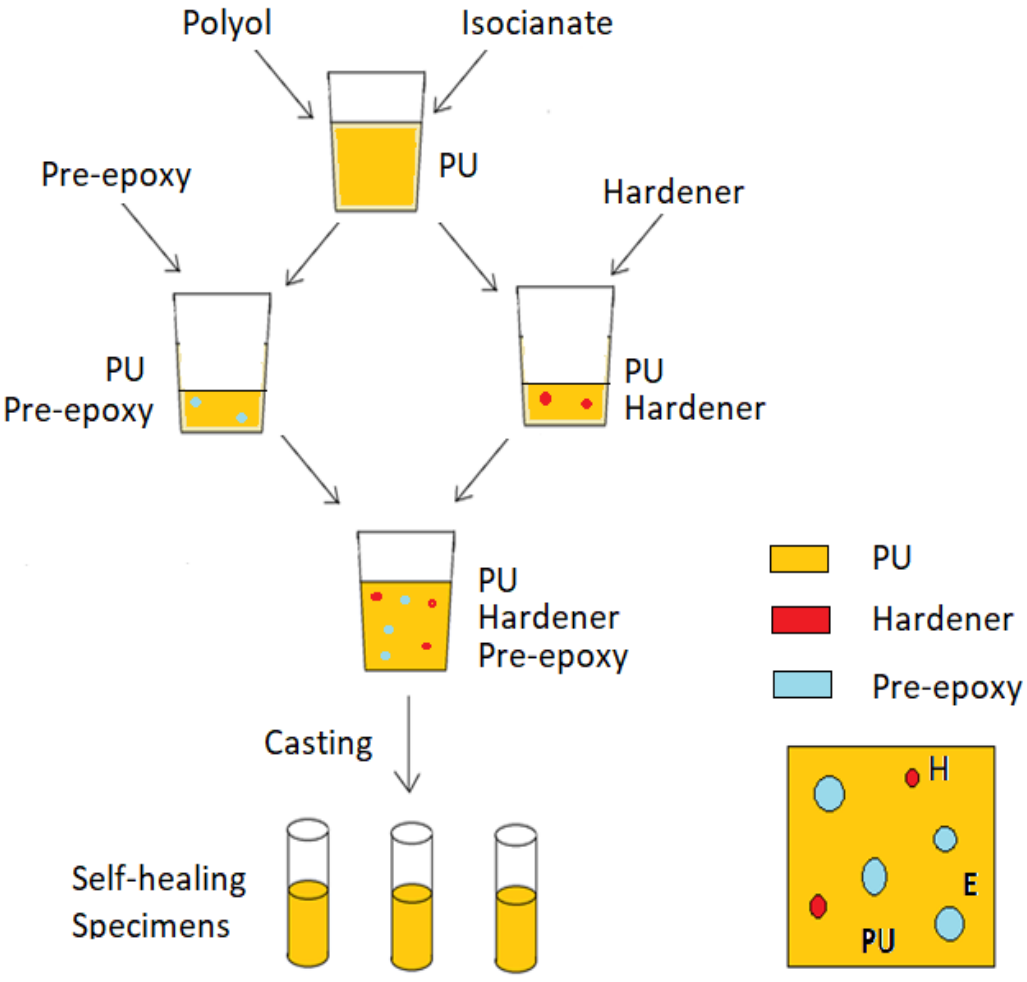

Figure 2.5: PU-epoxy based self-healing composite production

PU-MMA/PMMA Composites

Initially, polyurethane (PU) based matrix was prepared by by mixing 50 % liquid polyol and 50 % liquid isocianate. Then the polyurethane (PU) mixture was divided into two equal parts. One PU part was mixed with methylmetacrylathe (MMA) monomer and some fine PMMA powder, and the other PU mixture was mixed with the hardener (benzoyl peroxide, BPO) of the MMA. The two mixture were mixed about 2 minutes. Lastly, two mixtures (PU-MMA and PU-hardener) were mixed together and then poured into the mould. Fine PMMA powder was used as a carrier for the methylmetacrylathe (MMA) monomer droplets. Figure 2.6 illustrates the PU-PMMA/MMA based self-healing composite production steps.

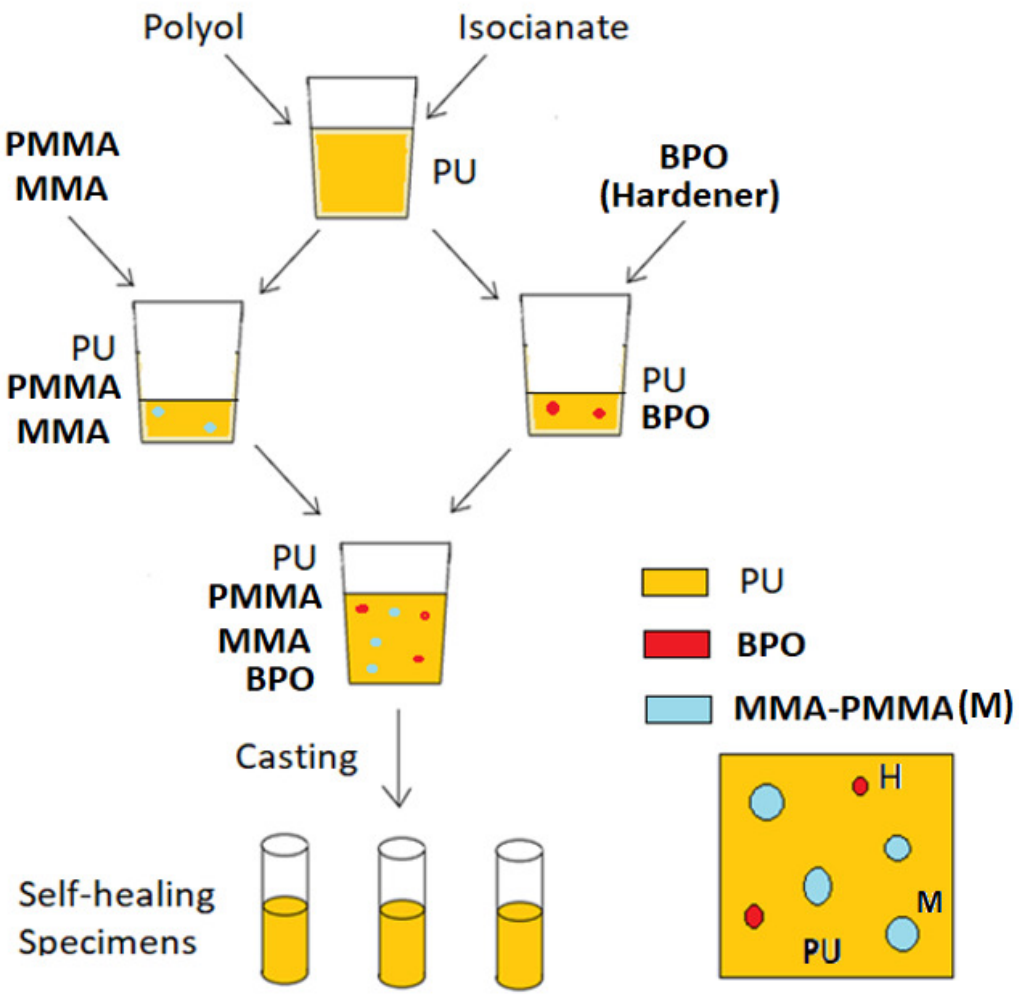

Figure 2.6: PU-PMMA/MMA based self-healing composite production

2.2. PRODUCTION OF METAL ALLOYS

Powder Metallurgy Method

In the the present thesis, Ti-Ni and Fe-Mn-Si based shape memory alloys were produced by powder metallurgy method, which consists of mechanical alloying (ball mill), pressing and sintering steps. Tables 2.1 and 2.2 show the compositions of Fe based and Ti-Ni based specimens.

Table 2.1: Compositions of the Ti-Ni based alloys

Alloy	Co	Ni	Ti	Sn
Ti-Ni		50	50	
Ti-Ni-Sn		50	45-47	3-5
Ti-Ni-Co	3-5	50	45-47	
Ti-Ni-Co-Sn	3-5	45-47	45-47	3-5

Table 2.2: Compositions of the Fe based alloys

Alloy	Fe	Mn	Ni	Ti	Si	Cr	Co
Fe-Mn-Si	70	25			5		
Fe-Mn-Si-Cr	65	25			5	5	
Fe-Ni-Co-Ti	88		5	5			2

In the the present thesis, Ti-Ni and Fe-Mn-Si based shape memory alloys were produced by powder metallurgy method, which consists of mechanical alloying (ball mill), pressing and sintering steps. Figure 2.7 shows the pictures of ball mill (mechanical alloying), hydraulic press, and tube furnace for sintering.

Figure 2.7: a) Ball mill and hydraulic press, b) sintering furnace

Shape Memory Training

In the present study, the sintering of the green specimens was carried out in vacuum in a horizontal type tube furnace (MTI GSL1500X, USA) at 1200 ºC for duration of 60 minutes. Then, the tube was removed out from the heating zone of the furnace, and samples were rapidly cooled. The cooling rate was about 1.0-3.0 ºC/s. Then, the specimens were aged for about 60 minutes at 400 °C temperature.

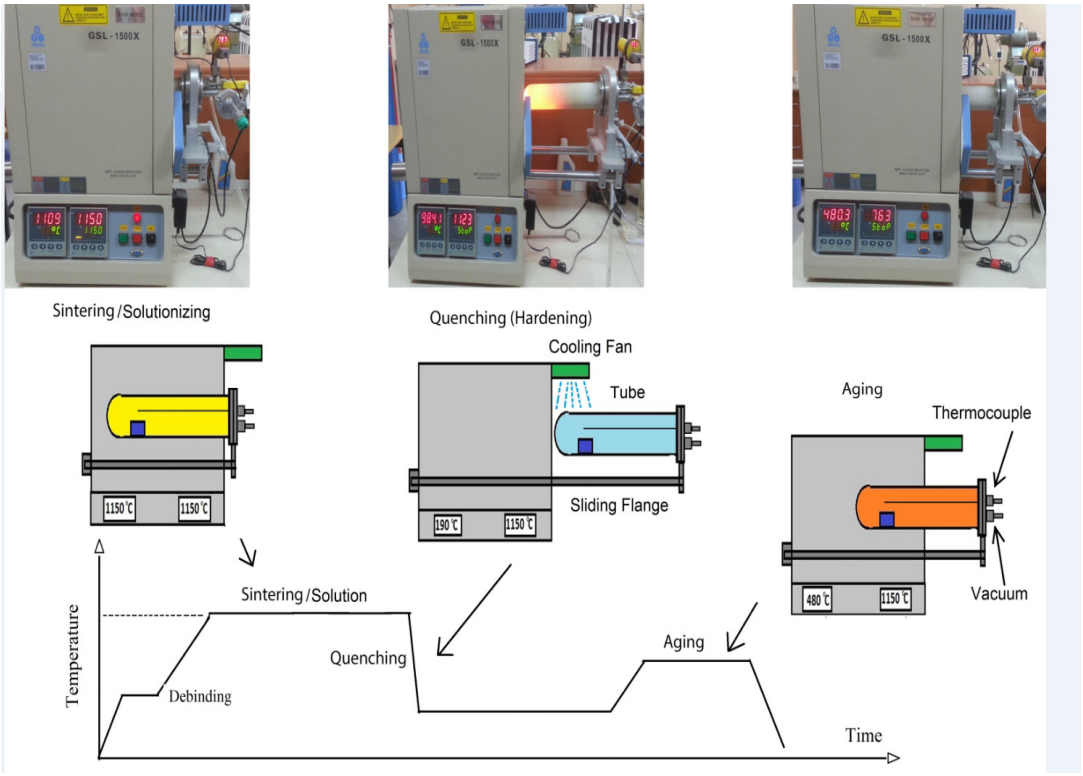

Figure 2.8: Shape memory training heat treatment

2.3. CHARACTERIZATION

Microstructure

The SEM (scanning electron microscope) device was used in order to investigate the microstructure (pore morphology, pore size and microstructural phases) of the specimens (FEI Quanta FEG 450).

X-ray diffraction (Rigaku 2200) was employed for the identification and evaluation of the phases in the microstructure of the alloys.

Corrosion experiments were conducted in SBF (simulated (artificial) body fluid). The SBF was included (in g/L) of 8.00 NaCl, 0.4 KCl, 0.1 $CaCl_2$, 0.1 $MgCl_2$, 0.07 Na_2HPO_4, 0.07 Na_2SO_4, 0.70 $NaHCO_3$, and buffer (tris) (Merck). Electrochemical corrosion tests were performed using a potentiostat (Interface 1000, Gamry).

Mechanical Properties

Tension/Compression

Mechanical properties (Young's (elastic) modulus and strength) of the materials was examined by performing tension-compression tests (Devotrans, Turkey).

Figure 2.9: Tension-compression test device

Ultrasonics

Mechanical parameters of the alloys was also evaluated by non-destructive based ultrasonic testing (USM Go, General Electric). Measurements were carried out by pulse-echo mode transducer having 4 MHz probe [10-12].

$$E = \rho V_T^{\,2} \frac{3V^2_L - 4V_T^{\,2}}{V_L^{\,2} - V_T^{\,2}} \qquad (1)$$

Strain Gauge Measurements

Maximum (principal) stress and strain values in the composite specimens were measured by strain gauges (BF350-3AA) with resistance of 350 Ω. Diemensions of the strain gauges were 7.4x4.4 mm, while sensitivity was 2.0-2.2.

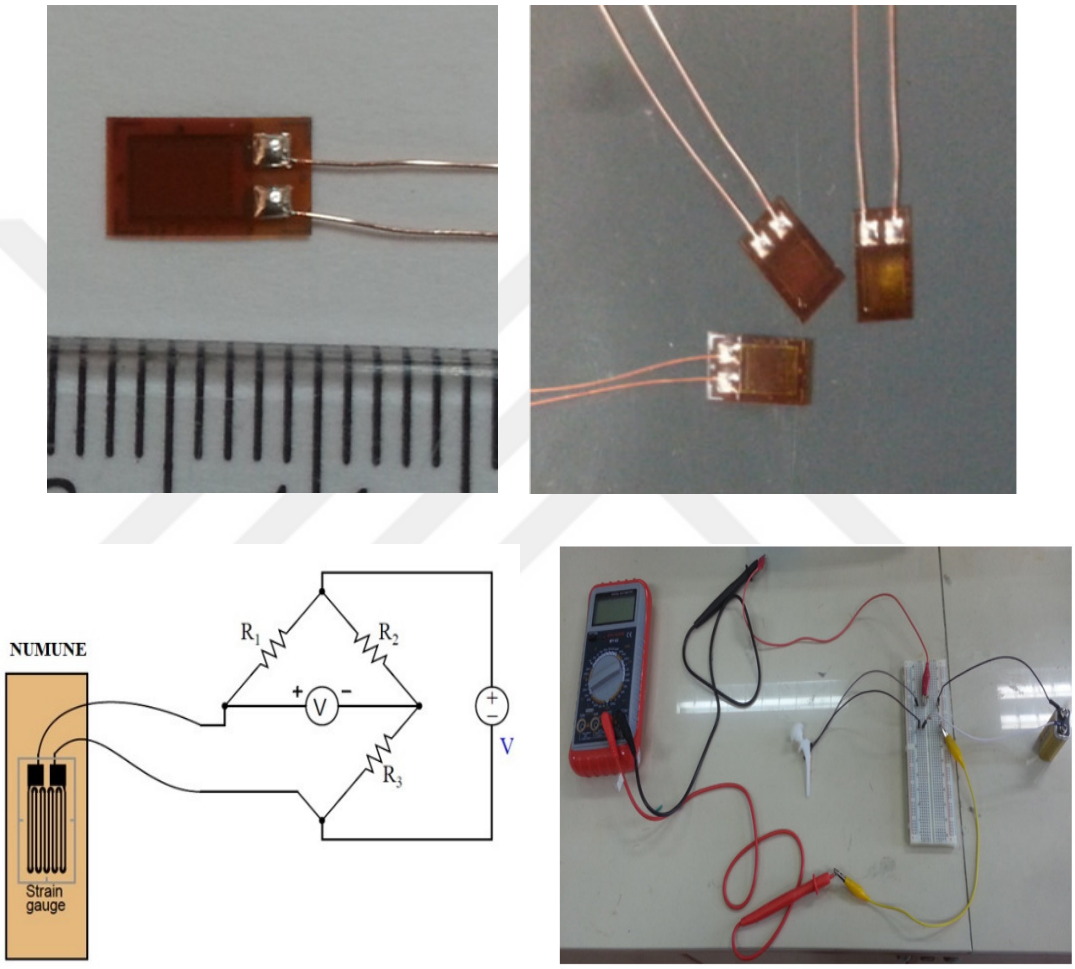

Figure 2.10: a) Strain gauges, b) rosette, c) Wheatstone bridge

3. RESULTS

3.1. POLYMER MATERIALS

Figure 3.1 shows the pictures of a) epoxy-CNT powder, b) PU-TiNi powder, c) PU-TiNi powder / epoxy-CNT powder based meta-material shaped shape memory composite specimens.

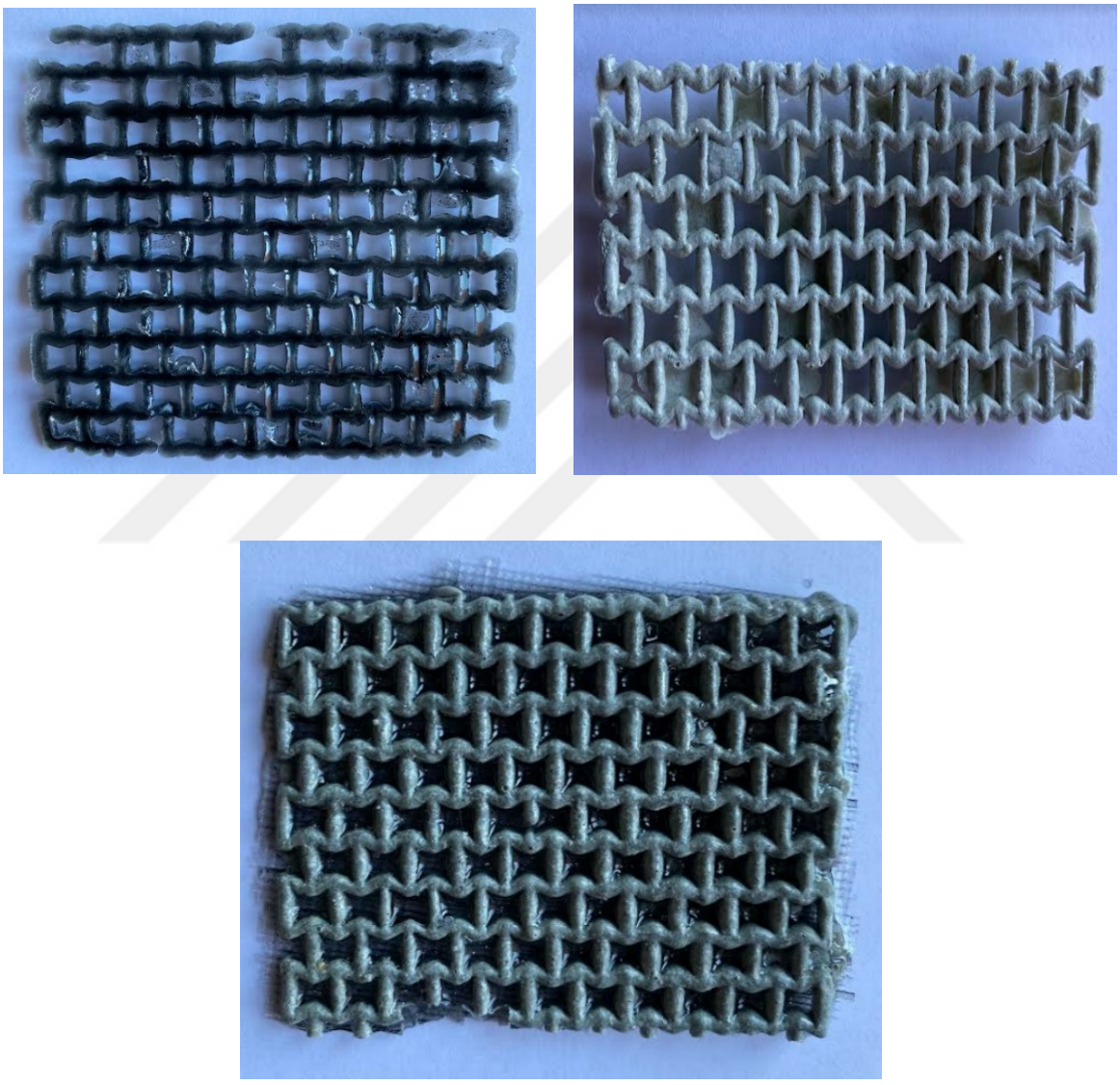

Figure 3.1: Pictures of a) epoxy-CNT, b) PU-TiNi, c) PU-TiNi / epoxy-CNT

Figure 3.2 shows the pictures of metamaterial shaped shape memory a) epoxy-TiNi powder, b) epoxy-TiNi-CNT powder composite specimens.

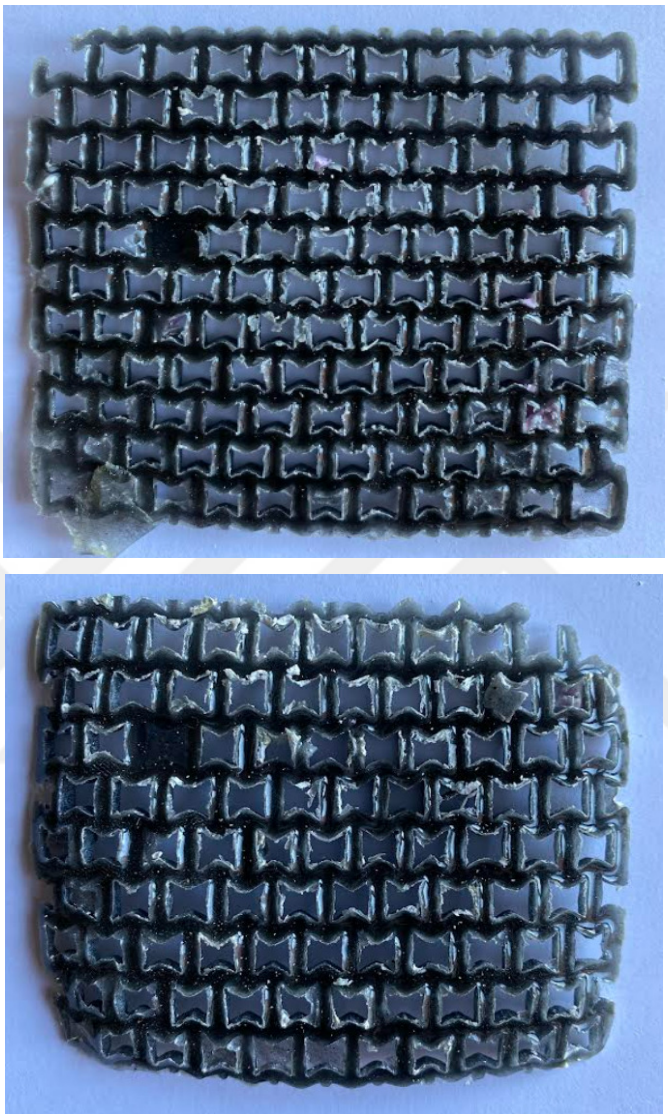

Figure 3.2: Pictures of a) epoxy-TiNi, b) epoxy-TiNi-CNT

Microstructure of Polymer Matrix Composite Materials

Figure 3.3 shows the SEM pictures of a) carbon nano tube (CNT) powder, and b) epoxy-TiNi powder-CNT powder composite specimen. As seen in the SEM image, there is an uniform distribution of the Ti-Ni and CNT powders in the epoxy matrix.

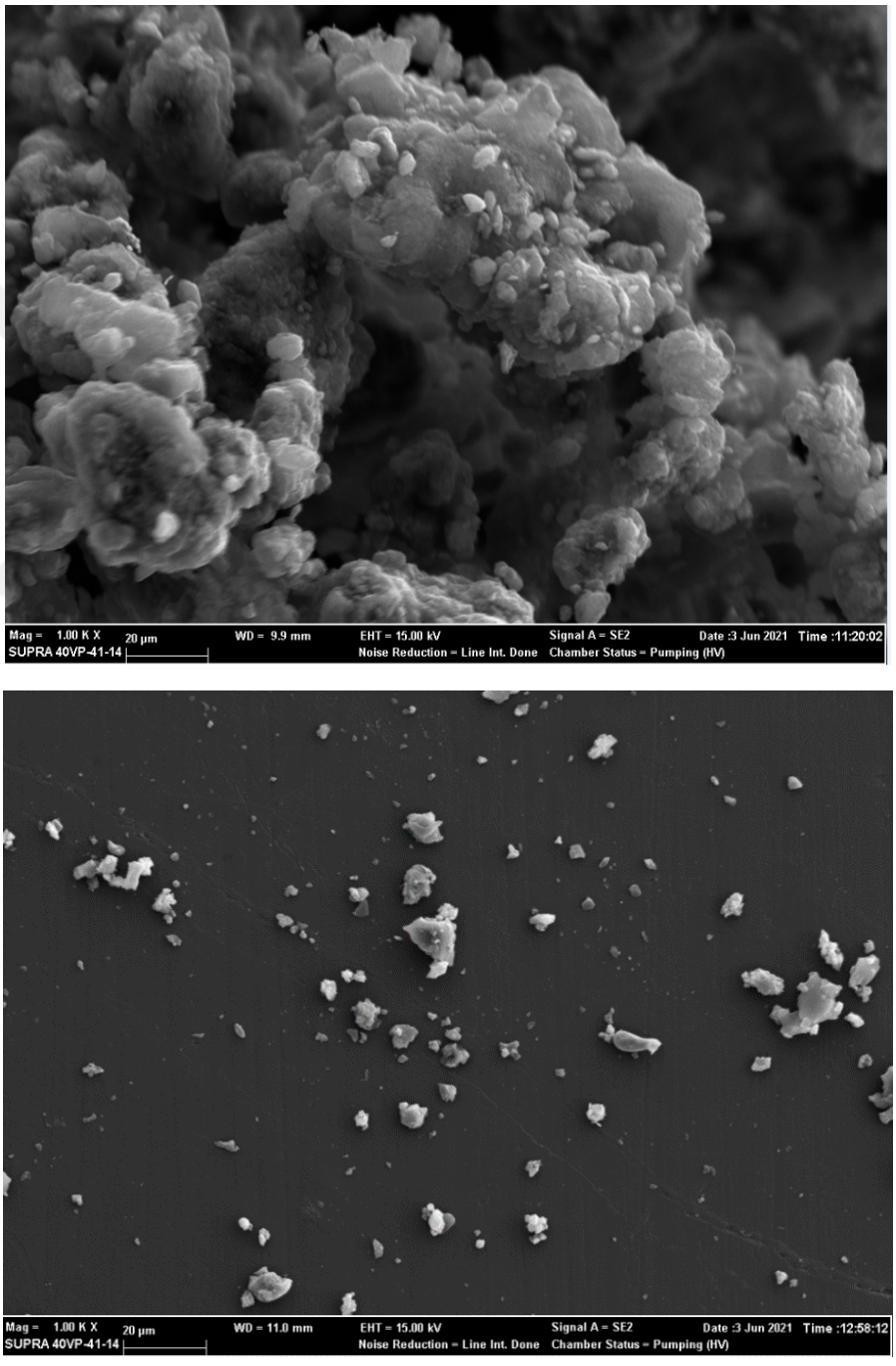

Figure 3.3: SEM pictures of a) CNT, b) epoxy-TiNi-CNT composite

Microstructure of Self-Healing Materials

Figure 3.4 shows the SEM and optical microscope pictures of the microstructure of the PU-based self-healing composite specimen. As seen, there is an uniform distribution of monomer droplets and its hardener in the solid PU matrix, as expected.

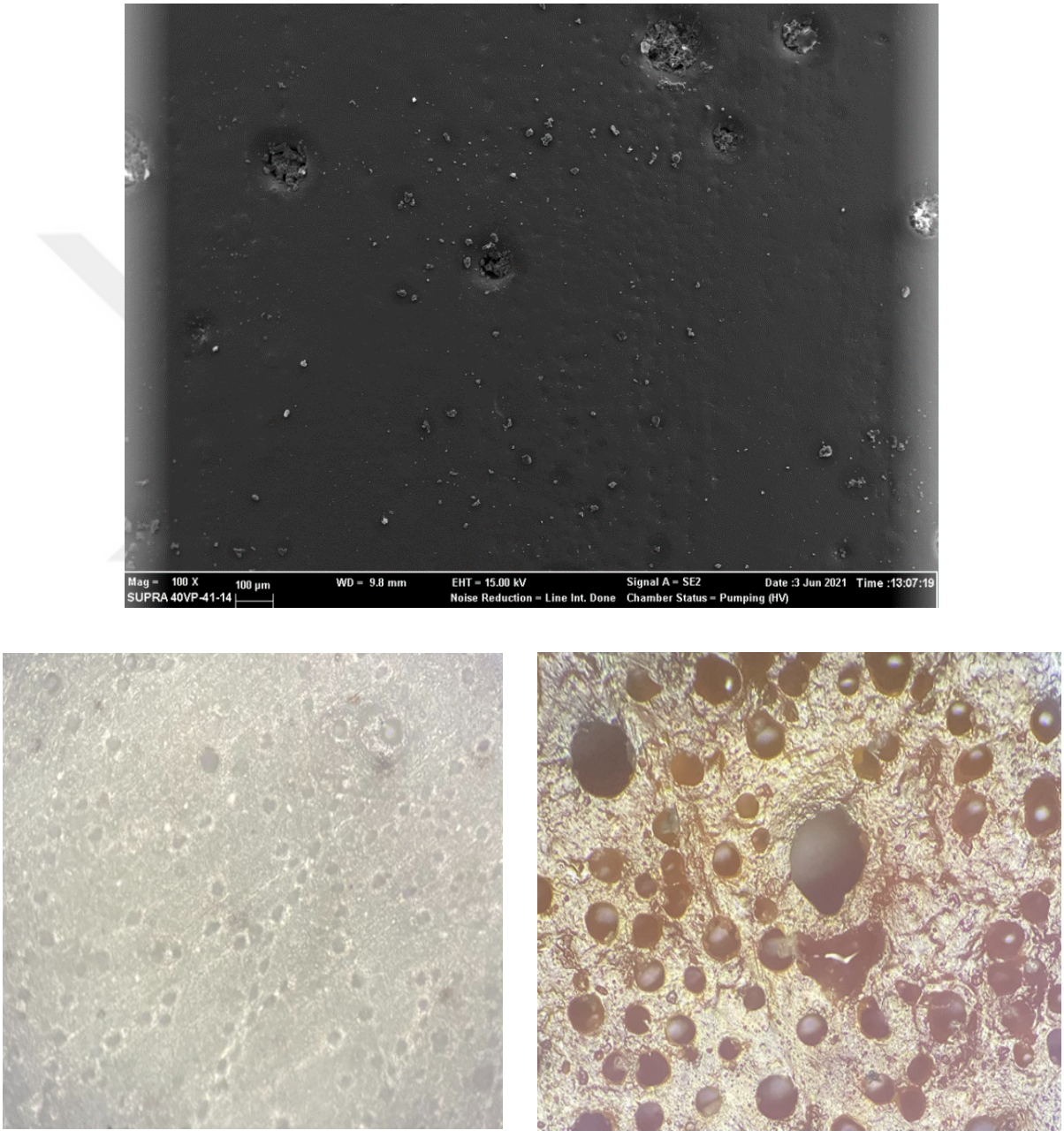

Figure 3.4: Microstructure of PU-based self-healing composite

Mechanical Properties

Figure 3.5 shown below illustrates the picture during the compression tests (vertical and horizontal) of the meta-material shaped polymer matrix composite specimen. Mechanical properties were different depend on the force/load direction. Compression strength was higher in vertical direction (lower photograph) than horizontal (upper photograph).

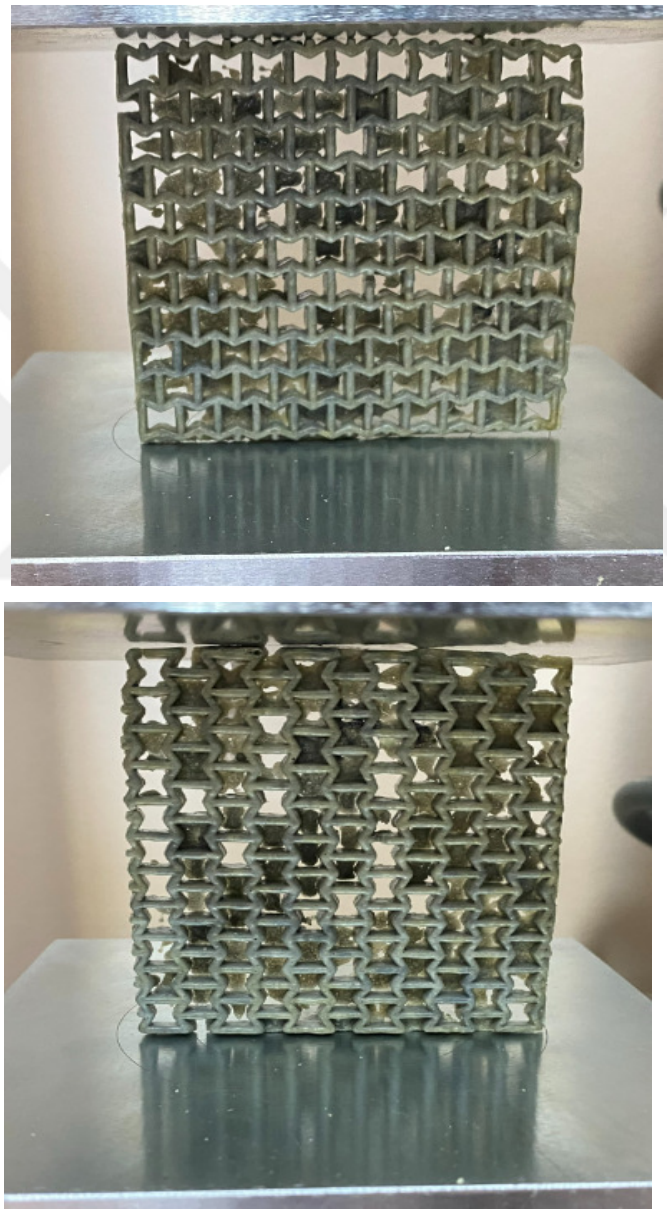

Figure 3.5: Photographs during compression tests of PU composites

Self Healing Materials

Figure 3.6 given below shows the screens of ultrasonic device during the tests. Screens of the sdevice of the elf-healing specimens before (with crack) and after healing (without crack) can be seen in the pictures. Firs and back-wall echo peaks and peak from crack can be seen in the screen of the ultrasonic device. In addition, peaks of the crack were decreased or completely eliminated, as a result of self-healing.

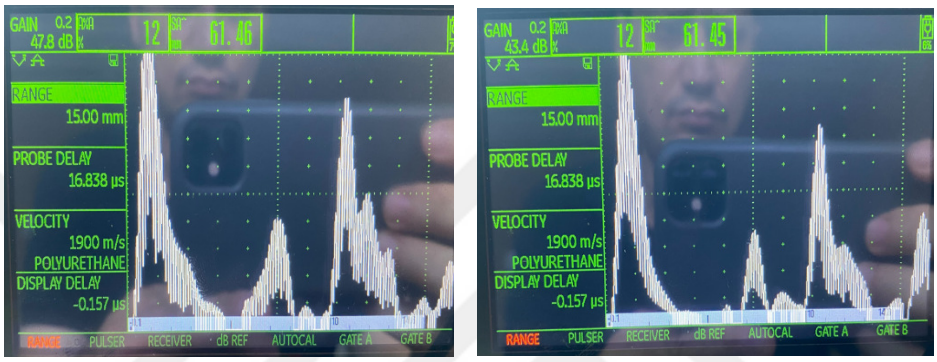

(a)

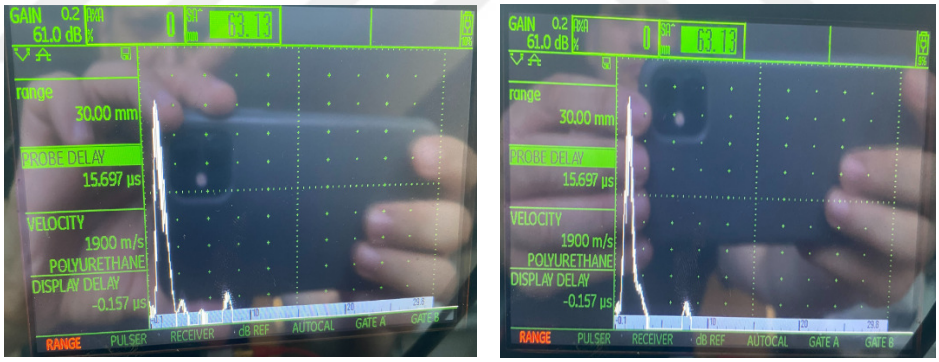

(b)

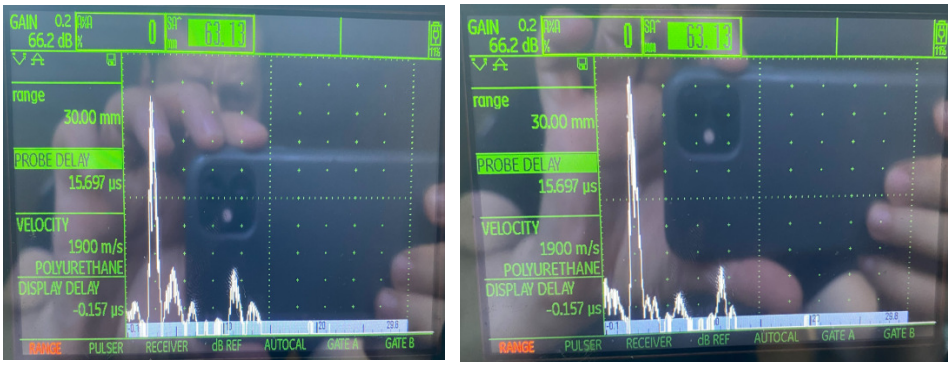

(c)

Figure 3.6: Ultrasonic device screen of self-healing materials

3.2. METAL ALLOYS

Microstructure

In the present study, shape memory Ti-Ni based specimens were produced by powder metallurgy method by using fine metal powders. Figure 3.7 given below exhibits the SEM pictures of the (a) Ni, (b) Ti, (c) Co, (d) Sn powders.

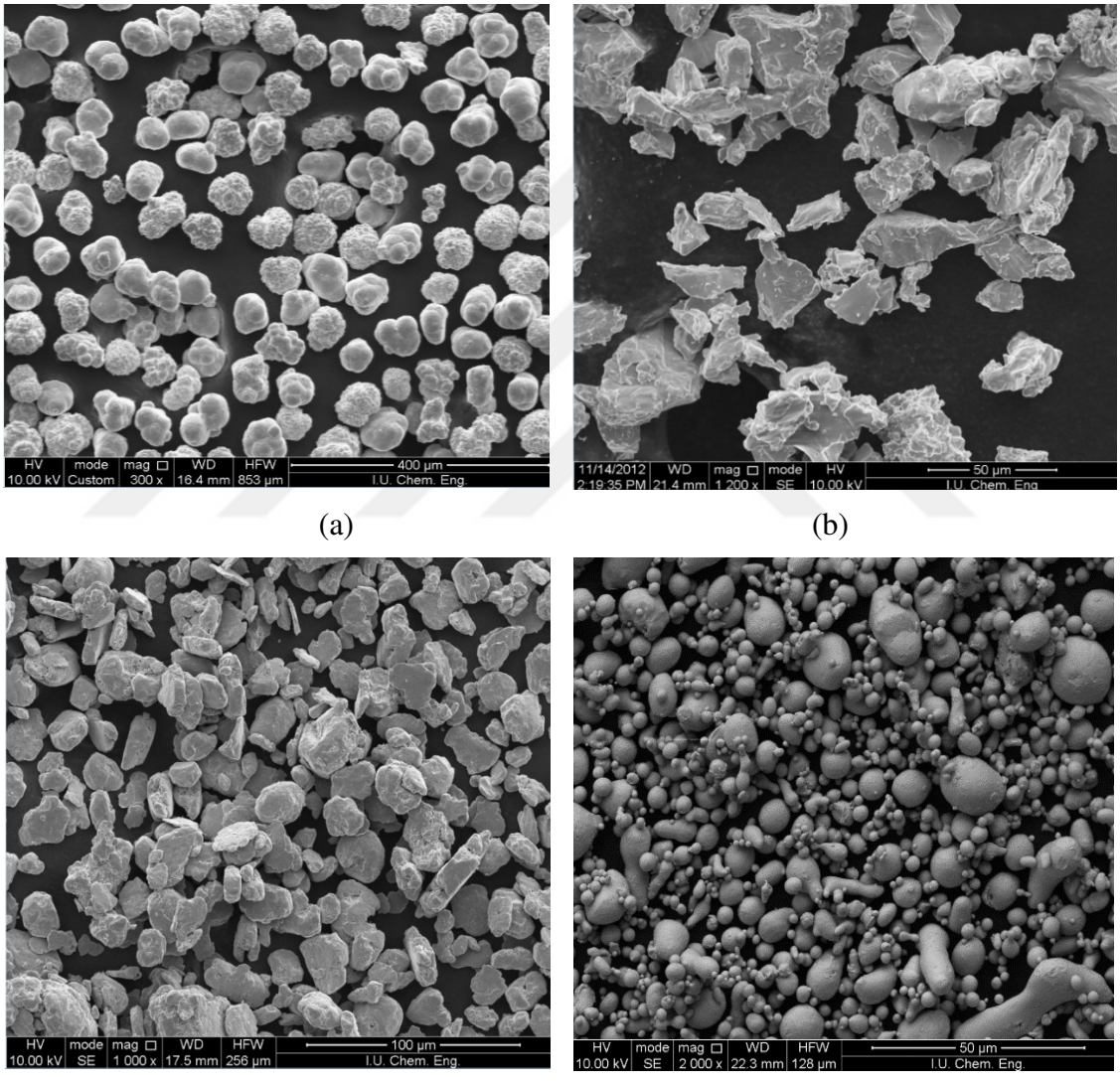

(a) (b)

(c) (d)

Figure 3.7: SEM picture of a) Ni, b) Ti, c) Co, d) Sn powders

In the present study, shape memory Fe based specimens were produced by powder metallurgy method by using fine metal powders. Figure 3.8 given below exhibits the SEM pictures of the (a) Fe, (b) Mn, (c) Si, (d) Cr powders.

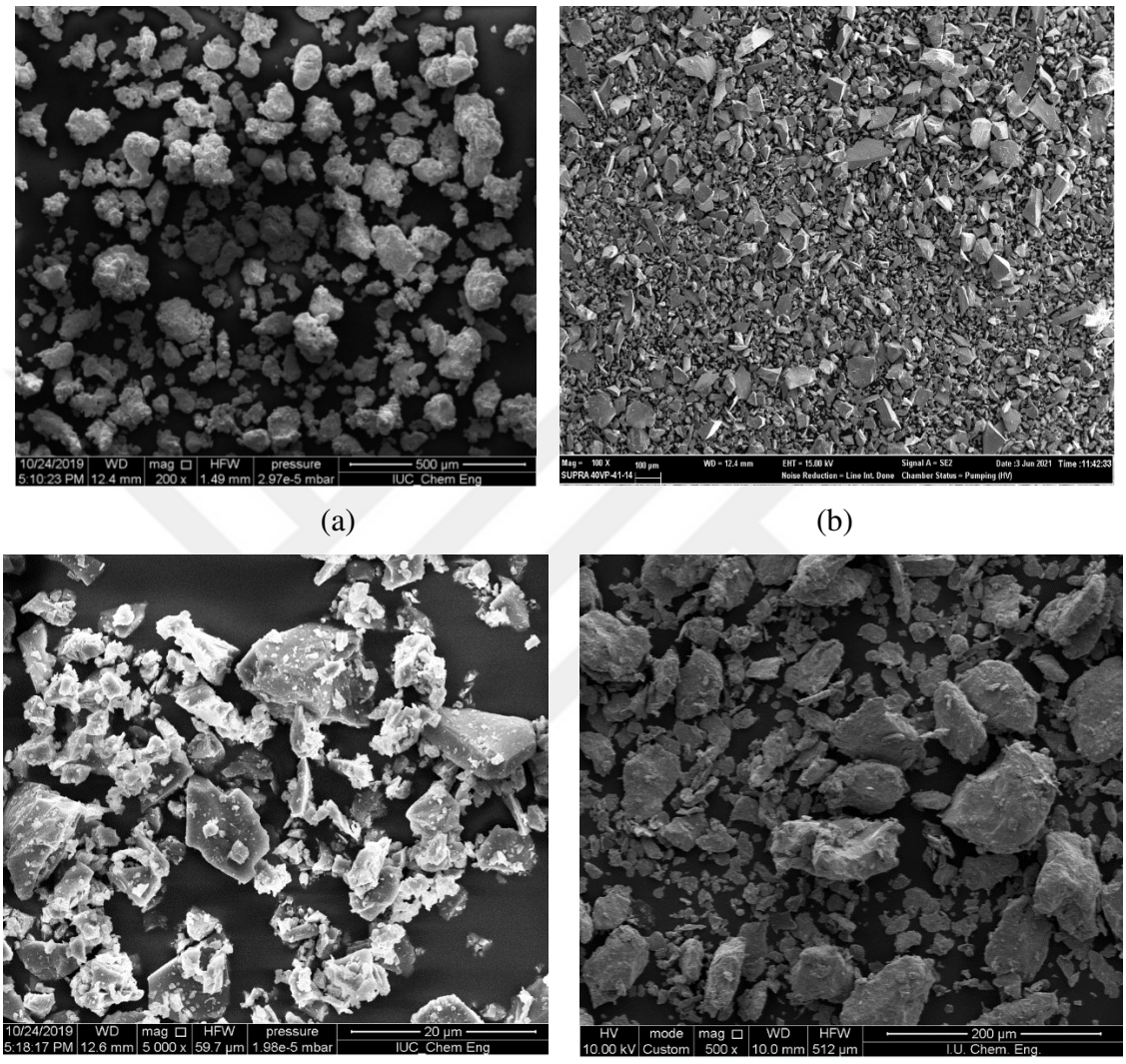

Figure 3.8: SEM picture of a) Fe, b) Mn, c) Si, d) Cr powder

Figure 3.9 given below shows the SEM picture of the microstructure of the sintered shape memory 45Ti-45Ni-5Co-5Sn alloy specimen. As seen from the Figure 3.9, there is a suitable sintering between the metal powder particles. In addition, there is no microcracks or macrocracks in the microstructure of the sintered alloy.

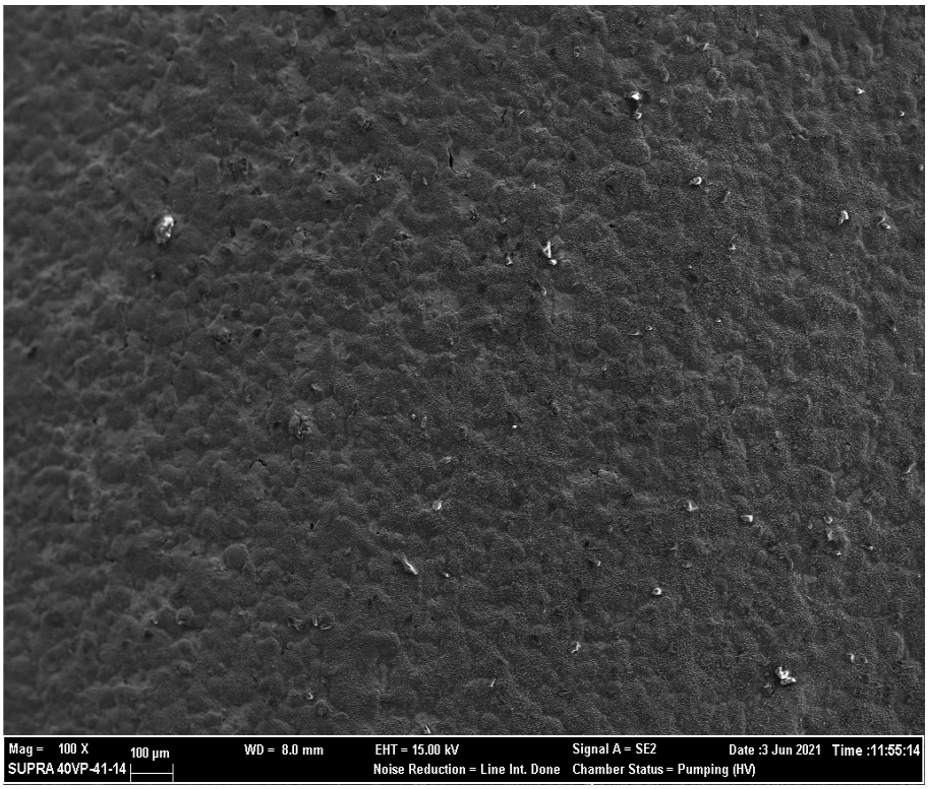

Figure 3.9: a) SEM picture of of sintered Ti-Ni alloy

Figure 3.10 given below shows the SEM picture of the microstructure of the sintered shape memory Fe-Mn-Si alloy specimen. As seen from the Figure 3.10, there is a suitable sintering between the metal powder particles. There is no macrocracks or microcracks in the microstructure of the sintered alloy.

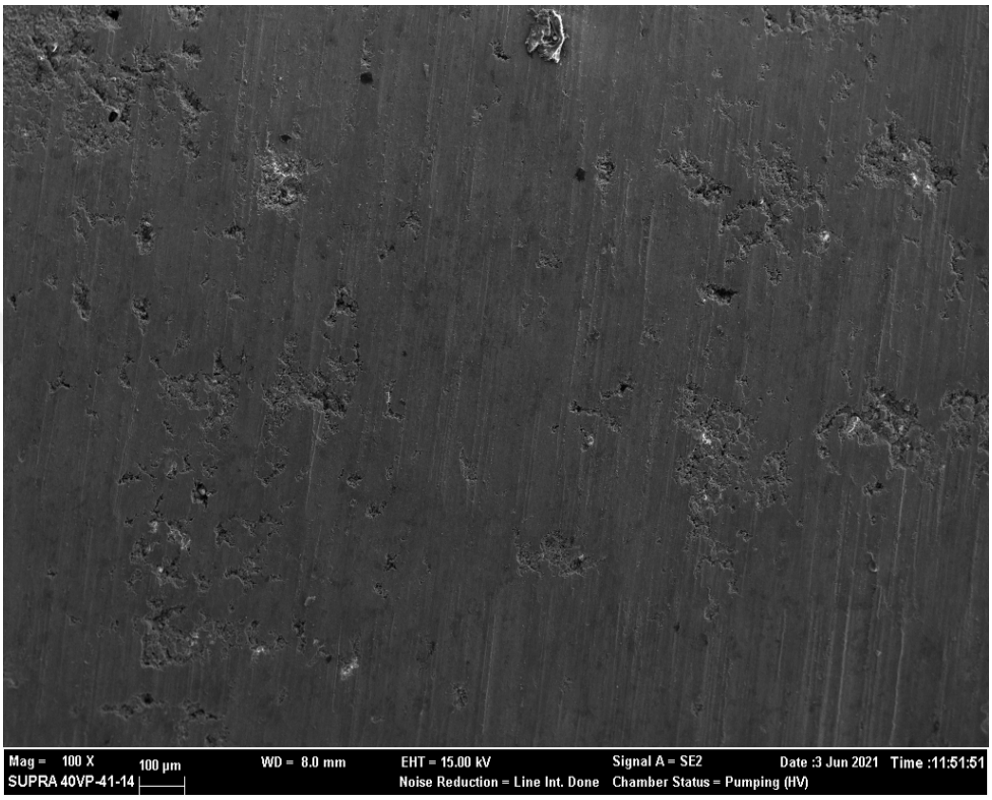

Figure 3.10: SEM picture of Fe-Mn-Si alloy

XRD Results

Microstructure of the shape memory Ti-Ni based materials was characterized by x-ray diffraction (XRD). Figure 3.11 given below illustrates the patterns of a) Ti powder, b) Ni powder, and c) sintered shape memory Ti-Ni-Co alloy.

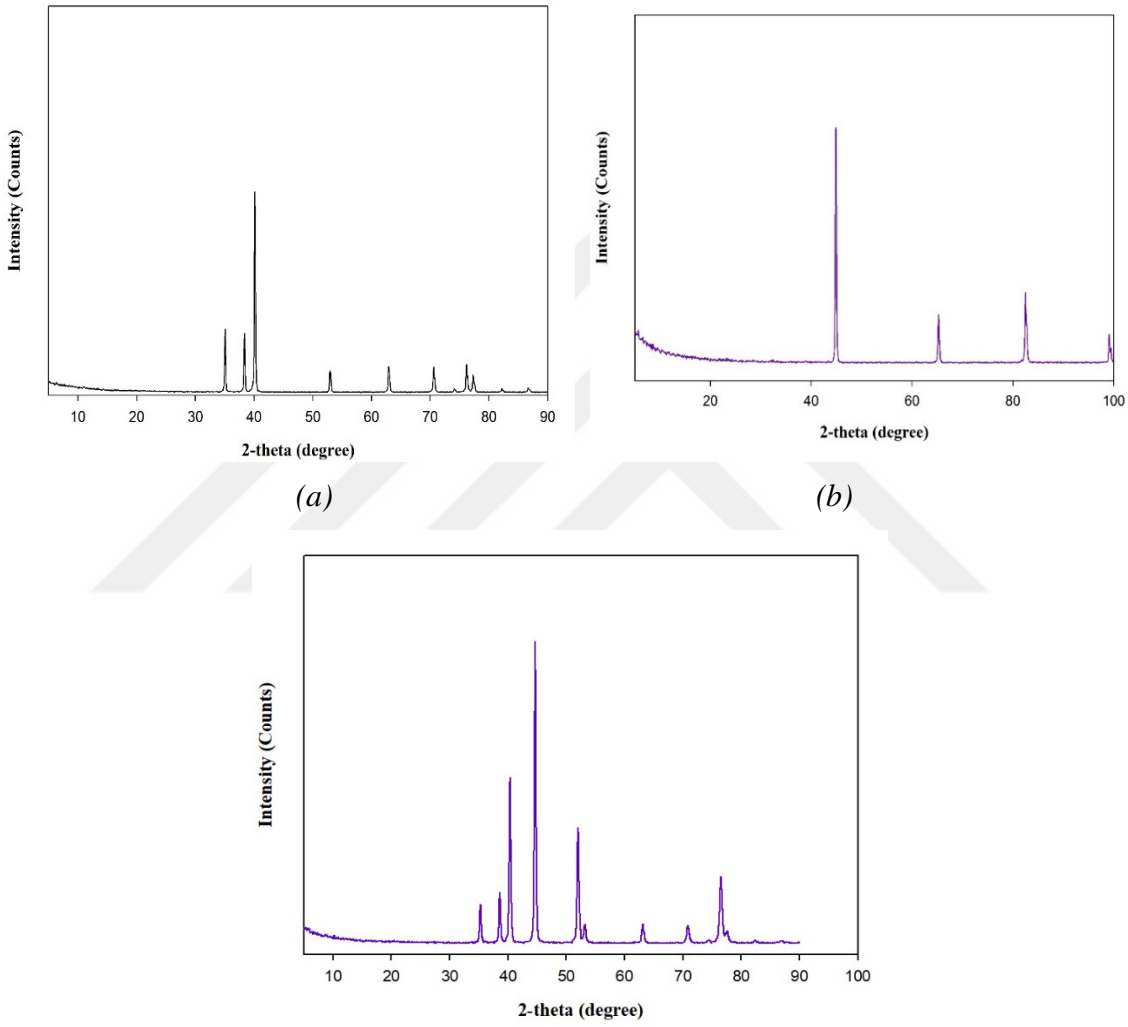

Figure 3.11: XRD results of the a) Ti powder, b) Ni powder, c) Ti-Ni-Co alloy

Microstructure of the Fe based shape memory materials was also characterized by the x-ray diffraction (XRD) study. Figure 3.12 given below illustrates the patterns of a) Fe powder, b) Mn powder, and c) sintered shape memory Fe-Mn-Si alloy.

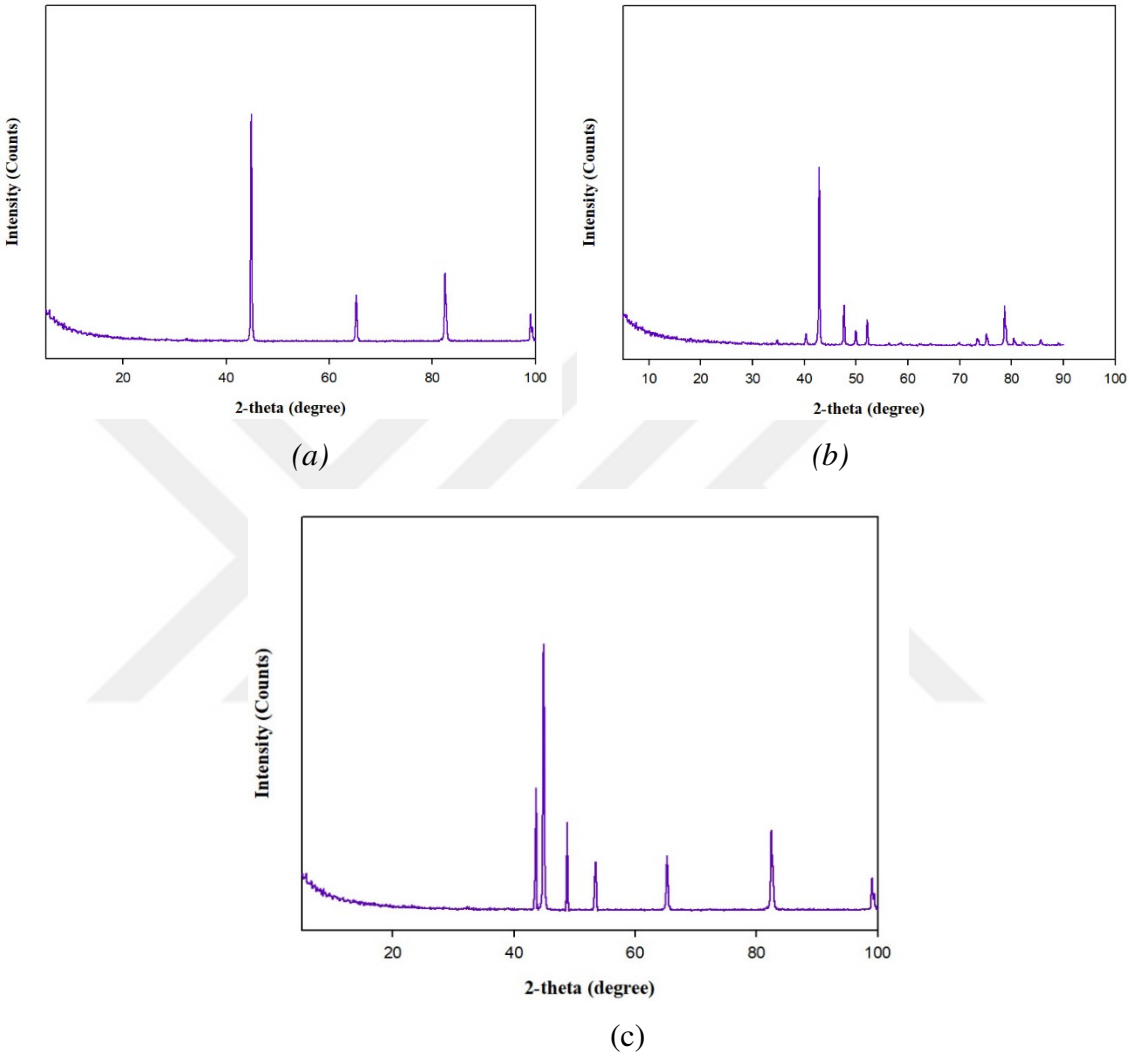

Figure 3.12: XRD results of the a) Fe powder, b) Mn powder, c) Fe-Mn-Si alloy

Mechanical Properties

Figure 3.13 given below shows the effect of aging temperature on the elastic modulus of the sintered shape memory 45Ti-50Ni-5Co samples. As shown in the Figure 3.13, optimum aging temperature was about 400 ºC. elastic modulus was slightly decreased after 400 ºC due to overaging.

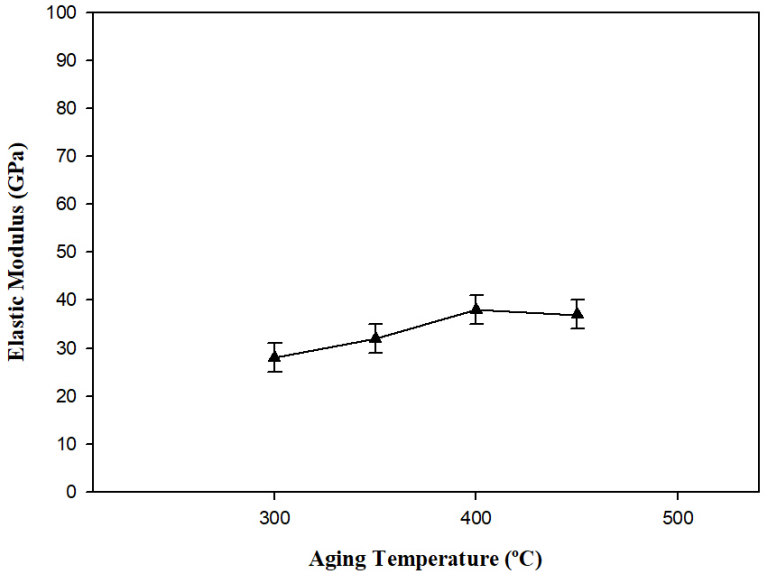

Figure 3.13: Effect of aging temperature on elastic modulus of TiNi specimens

Figure 3.14 given below shows the effect of aging temperature on the elastic modulus of the shape memory Fe-Mn-Si samples. As shown in the figure 3.14, increasing aging temperature slightly increased the elastic modulus of the specimens.

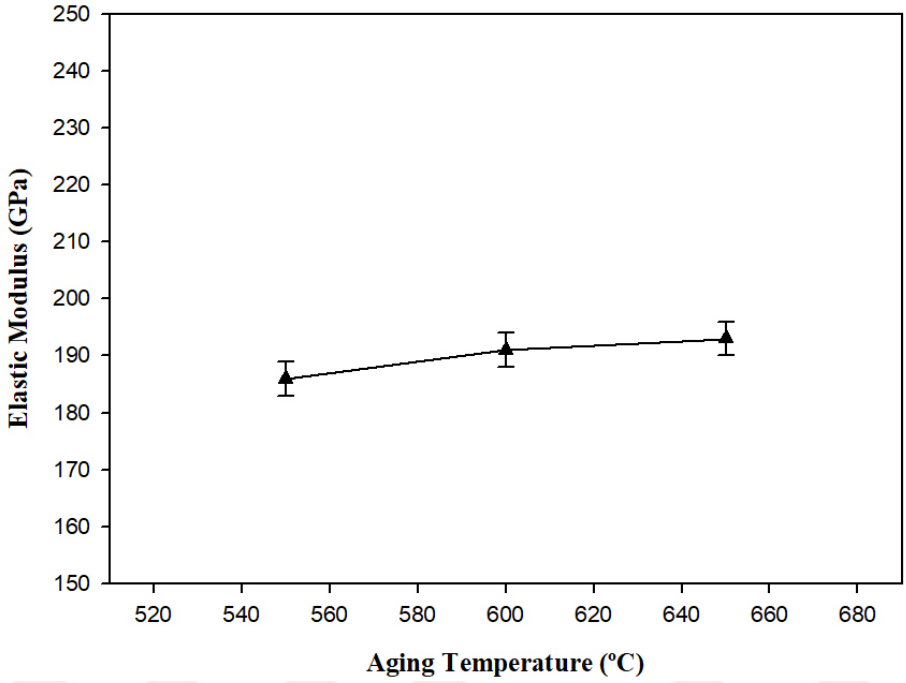

Figure 3.14: Effect of aging temperature on elastic modulus of Fe-Mn-Si specimens

Figure 3.15 illustrates the effect of temperature on the elastic modulus of the sintered shape memory 45Ti-50Ni-5Co alloy. Austenite-martensite phase transformation temperature of the sintered shape memory Ti-Ni-Sn based alloy was about 30 °C temperature. As the martensite and austenite phases have different elastic modulus values from each other, austenite-martensite phase transformation temperature of the alloy can be determined by the ultrasonic velocity measurements.

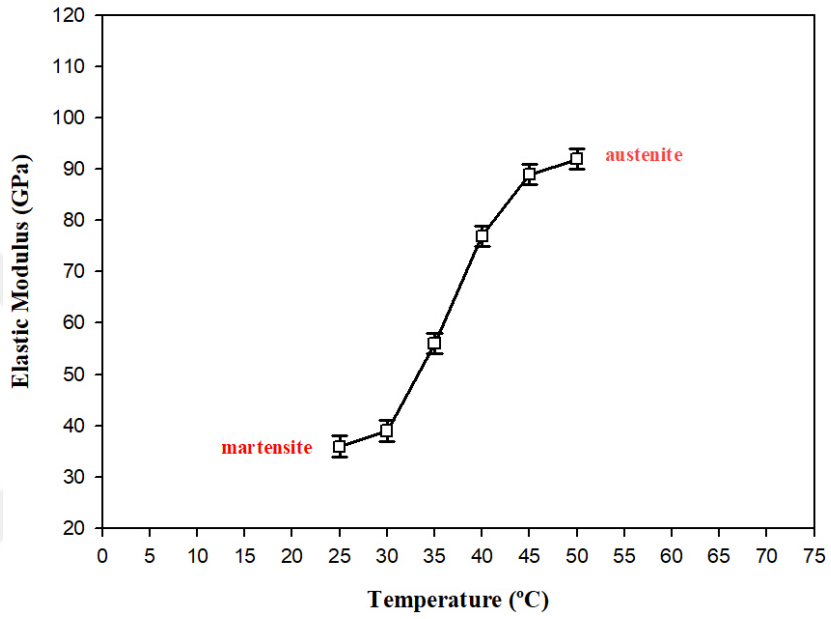

Figure 3.15: Effect of temperature on the elastic modulus of the Ni-Ti alloy

Figure 3.16 illustrates the effect of temperature on the elastic modulus of the sintered shape memory Fe-Mn-Si alloys. Transformation temperature of the sintered shape memory Fe-Mn-Si alloy was about 180-200 °C. As the martensite and austenite phases have different elastic modulus values from each other, martensite-austenite phase transformation temperature of the alloy can be determined by the ultrasonic velocity measurements.

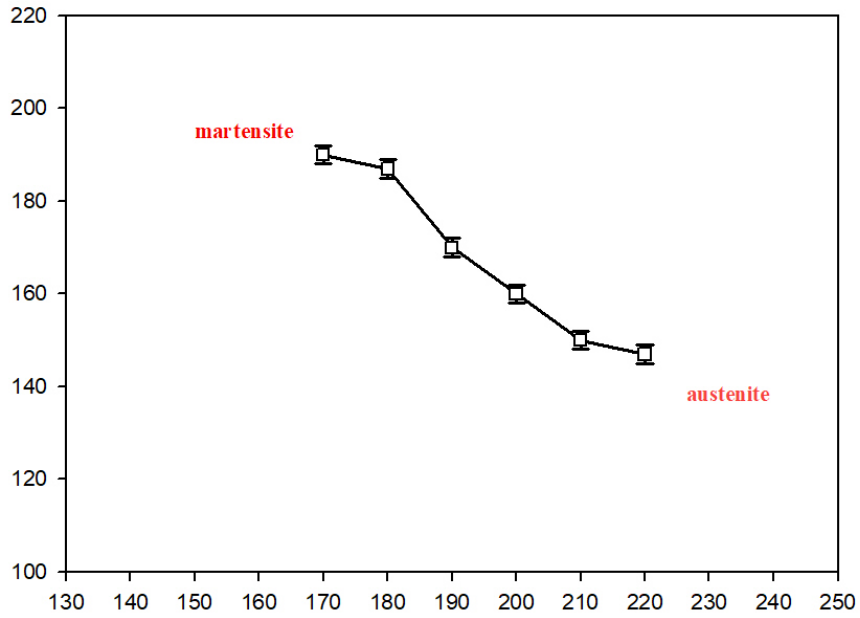

Figure 3.16: Effect of temperature on the elastic modulus of the Fe-Mn-Si alloy

4. DISCUSSION

In this thesis, development, production and characterization of several polymer matrix composite and metal based smart materials for coronary stent applications were done. Moulds, which were used in the production of reinforced polymer matrix composites, were produced by stereolithography based additive manufacturing method. Then, the polymer matrix composite materials were produced by alginate molding. Shape memory TiNi powder, carbon nano tube (CNT) powder, and carbon black powder reinforced polymer matrix composite materials were poured into the mould. In addition, mechanical metamaterial shaped TiNi powder, carbon nano tube (CNT) powder, and carbon black powder reinforced epoxy and polyurethane matrix composites were manufactured. In addition, polymer matrix composite materials with self-healing behaviour were produced and their self-healing behaviour was investigated. Shape memory Fe based alloys and Ti-Ni based alloys were produced by powder metallurgy technique for stent applications. Microstructure and mechanical properties of the materials were studied. In addition, nondestructive ultrasonic tests were used in order to characterize the elastic modulus and self-healing behaviour of the specimens.

In general, shape memory alloys are gruop of advanced engineering materials and show shape recovery behaviour to their pre-deformed first shape by heating or by removal of stress (load). Nitinol is a very popular advanced material in the several engineering applications. In general, nitinol (Ni-Ti alloys) shows shape memory effect and superelasticity (pseudoelasticity) effect. Self-healing materials are type of smart material. Self-healing can be described as the property of a group of engineering material that enables to heal micro-cracks intrinsically. A stent is a very small hollow tube-shaped medical device. Usually, stents can be employed in order to open a closed coronar veins of the human heart. In this study, shape memory metal (Ni-Ti based and Fe based) or polymer materials and polymer based self-healing materials were fabricated. NiTi based and metamaterial based shape memory materials were intended for coronary stent applications.

In the present thesis, stereolithography based additive manufacturing device was used to produce moulds for the metamaterial-shaped TiNi powder reinforced polymer matrix composite specimens. Alginate based replica (moulding) method was used for the production of the metamaterials shaped composite products. Alginate was used as a moulding (negative)

material. Reinforced polymer matrix composites were poured into the alginate mould and then the metamaterial shaped specimens were obtained.

Polyurethane (PU) and epoxy matrix composites were produced. TiNi powder, carbon nano tube (CNT), and carbon black powders were used as a reinforcement. Polyurethane (PU) was produced by mixing 50 % liquid polyol and 50 % liquid isocianate. After mixing, the reinforcements (TiNi, CNT, carbon black) were included to the liquid polymer and lastly the viscous mixture was poured into the mould. Epoxy was produced by mixing 65 wt.% liquid epoxy pre polymer and 35 wt.% liquid hardener. After mixing, the reinforcements (Ti-Ni, CNT, carbon black) were included to the liquid polymer and lastly the viscous mixture was poured into the mould.

In the preparation of the PU-epoxy based self-healing materials, firstly 50 % liquid polyol and 50 % liquid isocianate was mixed. Then the PU mixture was divided into two equal parts. One PU part was mixed with liquid epoxy pre-polymer, and the other PU mixture part was mixed with the liquid hardener of epoxy. Then, two mixture were mixed together. Lastly, two mixtures (PU-epoxy and PU-hardener) were mixed together and then poured into the mould.

In the preparation of the PU-MMA based self-healing materials, initially 50 % liquid polyol and 50 % liquid isocianate was mixed. Then the PU mixture was divided into two parts. One PU part was mixed with methylmetacrylathe (MMA) monomer and some fine PMMA powder, and the other PU mixture was mixed with the hardener (benzoyl peroxide) of MMA. The two mixture were mixed. Lastly, two mixtures (PU-MMA and PU-hardener) were mixed together and then poured into the mould. Fine PMMA powder was used as a carrier for the methylmetacrylathe (MMA) droplets.

In the the present thesis, Ti-Ni and Fe-Mn-Si based shape memory alloys were produced by powder metallurgy method, which consists of mechanical alloying (ball mill), pressing and sintering steps.

Microstructure of the sintered shape memory Ti-Ni based based specimen and shape memory Fe-Mn-Si alloy based specimens were studied by SEM. There was a suitable sintering between the metal powder particles. In addition, there is no microcracks or macrocracks in the microstructure of the sintered Ti-Ni alloys or Fe-Mn-Si alloys.

Effect of aging temperature on the elastic modulus of the sintered shape memory Ti-Ni samples was studied. Optimum aging temperature was about 400 ºC. Effect of aging temperature on the elastic modulus of the sintered shape memory Fe-Mn-Si samples was also studied. Optimum aging temperature was about 600 ºC.

Austenite-martensite phase transformation temperature of the sintered shape memory Ti-Ni alloy was about 30 °C temperature. Transformation temperature of the sintered shape memory Fe-Mn-Si alloy was about 180-200 °C. As the martensite and austenite phases have different elastic modulus values from each other, martensite-austenite phase transformation temperature of the alloy can be determined by the ultrasonic velocity measurements.

5. CONCLUSION AND RECOMMENDATIONS

In this thesis, development, production and characterization of several polymer matrix composite and metal based smart materials for coronary stent applications were done. Moulds, which were used in the production of reinforced polymer matrix composites, were produced by stereolithography based additive manufacturing method. Then, the polymer matrix composite materials were produced by alginate molding. Shape memory TiNi powder, carbon nano tube (CNT) powder, and carbon black powder reinforced polymer matrix composite materials were poured into the mould. In addition, mechanical metamaterial shaped TiNi powder, carbon nano tube (CNT) powder, and carbon black powder reinforced epoxy and polyurethane matrix composites were manufactured. In addition, polymer matrix composite materials with self-healing behaviour were produced and their self-healing behaviour was investigated. Shape memory Fe based alloys and Ti-Ni based alloys were produced by powder metallurgy technique for stent applications. Microstructure and mechanical properties of the materials were studied. In addition, nondestructive ultrasonic tests were used in order to characterize the elastic modulus and self-healing behaviour of the specimens.

In general, shape memory alloys are gruop of advanced engineering materials and show shape recovery behaviour to their pre-deformed first shape by heating or by removal of stress (load). Nitinol is a very popular advanced material in the several engineering applications. In general, nitinol (Ni-Ti alloys) shows shape memory effect and superelasticity effect. Self-healing materials are type of smart material. Self-healing can be described as the property of a group of engineering material that enables to heal micro-cracks intrinsically. A stent is a very small hollow tube-shaped medical device. Usually, stents can be employed in order to open a closed coronar veins of the human heart. In this study, shape memory metal (Ni-Ti based and Fe based) or polymer materials and polymer based self-healing materials were fabricated. NiTi based and metamaterial based shape memory materials were intended for coronary stent applications.

Microstructure of the sintered shape memory Ti-Ni based based specimen and shape memory Fe-Mn-Si alloy based specimens were studied by SEM. There was a suitable sintering between the metal powder particles. In addition, there is no microcracks or macrocracks in the microstructure of the sintered Ti-Ni alloys or Fe-Mn-Si alloys.

Effect of aging temperature on the elastic modulus of the sintered shape memory Ti-Ni samples was studied. Optimum aging temperature was about 400 ºC. Effect of aging temperature on the elastic modulus of the sintered shape memory Fe-Mn-Si samples was also studied. Optimum aging temperature was about 600 ºC.

Austenite-martensite phase transformation temperature of the sintered shape memory Ti-Ni alloy was about 30 °C temperature. Transformation temperature of the sintered shape memory Fe-Mn-Si alloy was about 180-200 °C. As the martensite and austenite phases have different elastic modulus values from each other, martensite-austenite phase transformation temperature of the alloy can be determined by the ultrasonic velocity measurements.

REFERENCES

[1] Şengör, İ., 2013, Shape memory polymer composites containing carbon based fillers, Yüksek Lisans Tezi, Ortadoğu Teknik Üniversitesi, Fen Bilimleri Enstitüsü, Kimya Mühendisliği.

[2] Velipaşaoğlu, M.S., 2020, The determination of fuctional fatigue life of high temperature shape memory alloys after cold Rolling process, Yüksek Lisans Tezi, Hacettepe Üniversitesi, Fen Bilimleri Enstitüsü, Makine Mühendisliği.

[3] Ren X., Das R., Tran P., Ngo T.G., Xie Y.M., 2018, Smart Mater. Struct. 27, 114-173.

[4] Jani J.M., Leary M., Subic A., Gibson M.A., 2014, Materials and Design. 56, 1078-113.

[5] Ma J., Karaman I., Noebe R.D., 2010, Materials and Design. 55, 257-315.

[6] Leng J., Lan X., Liu Y., Du S., 2011, Materials and Design. 56, 1077-1135.

[7] Yang Y., Urban M.W.., 2013, Chem Soc. Rev. 42, 7446.

[8] Ak, E., 2010, Stress and Deformation Analysis in Stents, Yüksek Lisans Tezi, Marmara Üniversitesi, Fen Bilimleri Enstitüsü, Makine Mühendisliği.

[9] O'Brien B., Zafar H., Ibrahim A., Zafar J., Sharif F., 2016, Annals of Biomedical Engineering. 44, 2, 523-535.

[10] Fu H., Zhao, H., Zhang Y., Xie J. 2017, Proceedia Engineering. 1505-1510.

[11] Tanaka Y. Kainuma R., Omori T., Ishida K., 2015, Materials Today. 485-492.

[12] Druker A.V., Perotti A., Esquivel I., Malarria J., 2015, Procedia Materials Science. 878-885.

[13] Aydoğmuş, T., 2010, Processing and Characterization of Porous Titanium Nickel Shape Memory Alloys, Doktora Tezi, Ortadoğu Teknik Üniversitesi, Fen Bilimleri Enstitüsü, Metalurji ve Malzeme Mühendisliği.

[14] Lee, N., 2018, Shape Memory Property of PCL/TPU Blends, Yüksek Lisans Tezi, Kocaeli Üniversitesi, Fen Bilimleri Enstitüsü, Polimer Mühendisliği.

[15] Söyler, A.U.., 2014, Fe-Mn-Si esaslı şekil bellekli alaşımların ileri toz metalürjisi yöntemleri ile üretilmesi, Doktora Tezi, İstanbul Teknik Üniversitesi, Fen Bilimleri Enstitüsü, Metalurji ve Malzeme Mühendisliği.

[16] Lee K.H.S, 2018, App Sci., 8, 730.

[17] Yuan S., Chua C.K., Zhou K., 2019, Adv. Mater. Tech., 4, 1800419.

[18] Wang H., Zhang Y., Lin W., Qin Q.H., 2020, Computational Materials Science, 171, 109232.

[19] Jabur A.S.., Al-Haidary J.T.., Al-Hasani E.S., 2013, Journal of Alloys and Compounds, 578, 136-142.

[20] Eda T., Khantachawana A., Umeda J., Kondoh K., 2019, Materials Transactions, 60, 8, 1583-1590.

[21] Liu B., Zheng Y.F., Ruan L., 2011, Materials Transactions, 65, 540-543.